CHAPTER I

Introduction

CHAPTER-I

INTRODUCTION

1. INTRODUCTION TO NANOTECHNOLOGY

The nano-science and nanotechnology are relatively growing in trend and displaying extensive activities in various scientific research fields. They have their origin in the idea of some researchers of the last century. The word "**Nano**" derived from the Greek word "Nanos" and it means dwarf or highly small. The nanoscience and technology are described by several meaning, which are usually interchangeable. The nanotechnology could be described as, "The science associating synthesis, characterization, designing and application of materials which are distinguished by one dimension in the nanometer range" [1]. Nanotechnology is thus described as having the following characteristics:

- Nanotechnology demands research and technology evolution at the 1 nm to 100 nm scale range.
- Nanotechnology produces and utilizes structures that have unique properties because of their size in small-scale level [2].

Nano-science is the investigation on manipulation of materials at atomic, molecular and macromolecular scale levels, where properties vary remarkably from those at a larger scale level [3].

Nowadays, the discipline of the nanoscience and nanotechnology are being quickly developed and getting greatly invested in most of the developed and developing countries.

1.1. NANOMATERIALS

Materials with an average grain size less than 100 nanometers are generally described as nanomaterials [4] or the material that contains nanoparticles, and having advanced properties such as higher strength and lower weight [5]. Nanometer sized materials form a bridge between atomic, molecular and bulk systems. The enhanced size and shape dependent properties of nanomaterials are extremely great compared

with their bulk counterparts. Nanomaterials are of having great attention because of its unique magnetic, optical, electrical, and other properties. These unique properties of the nanomaterials have the ability for huge impacts in medicine, electronics and other fields [5]. Nanomaterials have a high surface area to volume ratio than their bulk counterparts, which can lead to high chemical reactivity. It is possible to synthesize nanostructure materials, in various forms like powder, thin films, quantum wells, quantum wires, quantum dots, etc through various synthesis techniques.

1.1.1. Classification of nanomaterials

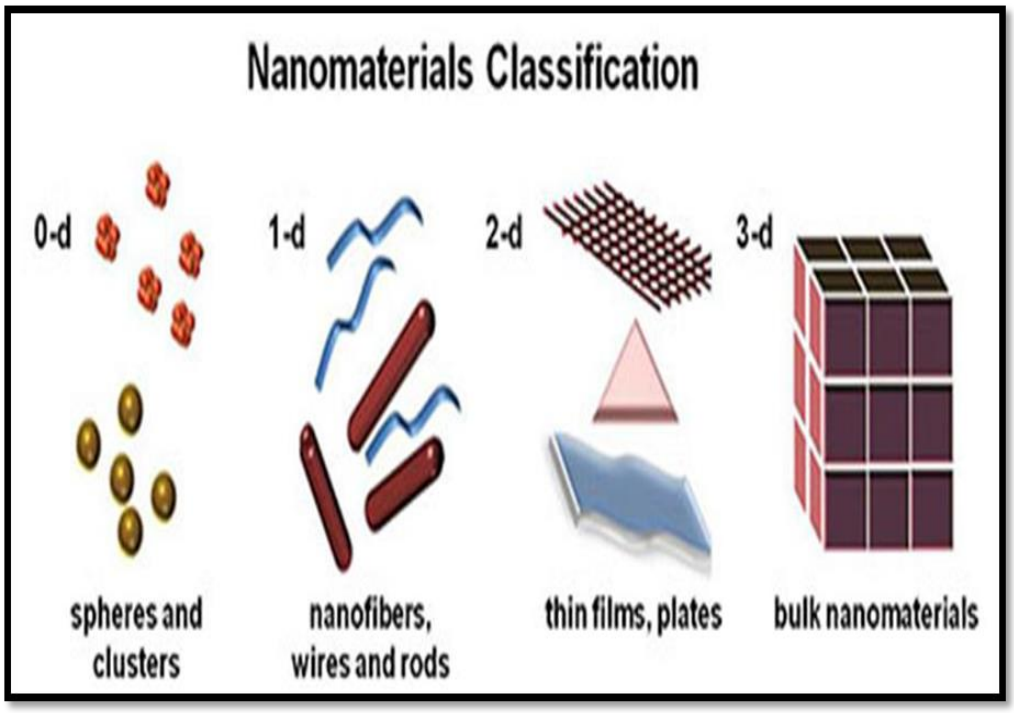

(a) **(b)** **(c)** **(d)**

Figure 1.1 Classification of Nanomaterials (a) 0-D spheres and clusters, (b) 1-D nanofibers, wires, and rods, (c) 2-D films, plates, and networks, (d) 3-D nanomaterials

Nanomaterials are significantly small in size (100 nm or less) and also having at least one dimension in the nanoscale level. Nanomaterials can be classified as one dimension (eg. surface films), two dimensions (eg. strands or fibres), and three dimensions (eg. particles) based on their number dimensions in the nanoscale level. Nanomaterials can also occur in single, fused and agglomerated forms with the tubular,

spherical and irregular shapes. Typical kinds of nanomaterials include dendrimers, quantum dots, nanotubes and fullerenes. Figure 1.1 displays the classification of nanomaterials. According to the scientist Siegel, Nanostructured materials are classified as

- **Zero dimensional nanomaterials**
- **One dimensional nanomaterials**
- **Two dimensional nanomaterials**
- **Three dimensional nanomaterials**

Nanomaterials have applications in the discipline of nano-technology, and show various physical chemical properties from normal chemical elements (i.e., nano silver, carbon nanotube, fullerene, photo-catalyst, nano carbon, silica) [5].

1-D Nanomaterials

Nanomaterials with one dimension in the nanometer scale are conventionally thin films or surface coatings. One dimension nanomaterials are widely present in the circuitry of computer chips and the antireflection and hard coatings on eyeglasses. These have been widely employed in the field of electronics, chemistry, and engineering [6].

2-D Nanomaterials

Nanomaterials with two dimensions in the nanometer scale are known as 2-D nanomaterials which include 2-D nanostructured films, or nanopore filters and are employed for small particle separation and filtration. Asbestos fibers are an ideal example of 2-D nanomaterials [6].

3-D Nanonmaterials

Material structures that are nanoscaled in all three dimensions are defined as 3-D nanomaterials, which include thin films synthesized under conditions that produce atomic-scale porosity, free nanoparticles and colloids with different morphologies [6].

1.2. SYNTHESIS OF NANOMATERIALS

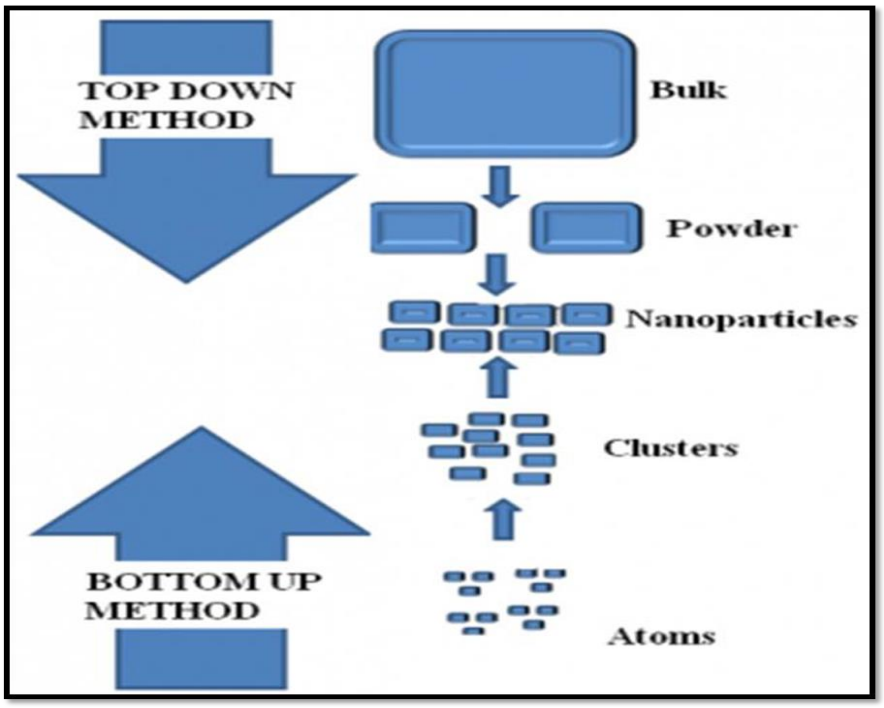

Figure.1.2. Synthesis of nanomaterials

For the synthesis of nanoparticles, the synthesizing mechanisms need to be optimized properly and the resulting nanoparticles have the following characteristics [7]: Identical size of all particles, identical shape, identical chemical composition and crystal structure and individually dispersed with no agglomeration. There are plentiful numbers of techniques to synthesize the nanomaterials which are classified into two techniques "top down approach and bottom up approach" as shown in the Figure.1.2. Ball milling and solid state route comes in the class of top down approach, while wet chemical methods like co-precipitation, sol-gel etc. come in the class of bottom up approach.

1.3. NANOPARTICLES

A nanoparticle is the most basic component in the formation of a nanostructure material, and it is significantly smaller than the world of day to day objects that are defined by Newton's laws of motion, but larger than an atom or a molecule that are executed by quantum mechanics. Typically, the size of a nanoparticle lies in the range between 1 to 100 nm with at least in one of the three desirable dimensions. In this range of size, the physical, chemical and biological property of the nanoparticles varies in

typical procedures from the properties of both definite atoms/molecules and of the associating bulk materials. Nanoparticles with a distinctly ordered alignment of atoms or ions are named as nanocrystallites. Nanoparticles can be formed in various morphologies such as cylinders, spheres, tubes, platelets etc. For example, metallic nanoparticles have various physical and chemical properties such as higher specific surface areas, lower melting points, specific optical properties, specific magnetization and mechanical strengths from bulk metals. These properties make metal nanoparticles as an attractive material in variety of industrial applications [8].

1.3.1. Types of nanoparticles

Nanoparticles can be widely classified into two,

- Organic nanoparticle
- Inorganic nanoparticle

Carbon nanoparticles such as fullerenes are known as organic nanoparticles while the magnetic nanoparticles, noble metal nanoparticles such as silver, gold and semiconductor nanoparticles such as titanium oxide and zinc oxide are known as inorganic nanoparticles. Among them, inorganic nanoparticles such as noble metal nanoparticles (silver and gold) exhibit a predominant material property with effective functionality. Due to the size characteristics of the nanoparticles, it has a significant role in chemical imaging of drugs and drug agents. Inorganic particles have also been employed as promising tools for medical imaging of diseases [9].

1.3.2 Properties of nanoparticles

Bulk materials have stable physical and chemical properties despite of its size. But in the case of nanoparticles, the size often dominates the physical and chemical properties. Thus, as the size of the material approaches the nanoscale level, the property of the material varies and also the percentage of atoms on the surface of the materials becomes significant. For bulk materials, the percentage of atoms on the surface of the materials becomes insignificant [6].

Optical properties

Nanoparticles have extraordinary optical properties as they are small enough to encircle their electrons and cause quantum effects. One example for the optical property of nanoparticle is that the gold nanoparticles emerge as a deep red to black colour in aqueous solution.

Mechanical properties

Due to the nanometer size, most of the mechanical properties such as elastic modulus, hardness, scratch resistance, fracture toughness and fatigue strength etc of the nanomaterials are quietly different from the bulk materials. An enhancement in the mechanical properties of nanoparticles may be due to the modification in the structural perfection of the materials. The value of the elastic constant of nanocrystalline material is found to be decreased by 30% or less, which may due to the enhancement in the average inter-atomic space value [10-11].

Thermal properties

Most of the properties such as electrical, magnetic, optical and mechanical properties of the nanoscale materials are well investigated. But, the thermal property of nanoparticles is only less studied due to the difficulties of practically analysing and controlling the thermal transport in nanoscale level dimensions. Atomic force microscope (AFM) has been employed to analyze the thermal transport of nanostructure materials with high spatial resolution [12]. In non-metallic material structure, the thermal energy is effectively carried by phonons, which have an extensive variation in the mean free paths and frequency. For macroscopic materials, the dimension is more sufficient to describe a local temperature in respective region within the material structures, so that the thermal transport properties of the system is based on temperature dispersion of the materials. In the case of nanomaterials, the dimension is found to be considerably small to describe a local temperature [12].

Formation of suspensions

Another eminent physical property of nanoparticles is their potentiality to form suspensions. The formation of suspension is possible only if the interaction between the particle surface and solvent is strong enough to defeat density differences. In the case of

bulk materials, the interaction between the particle surface and solvent is possible only if the material is either floating or sinking in a liquid.

1.4. APPLICATIONS OF NANOTECHNOLOGY

Nowadays, a life without nanoscience and technology is really tough to imagine. Nanotechnology is assisting to significantly upgrade many technological and industrial sectors such as homeland security, information technology, transportation, medicine, food safety, energy and environmental science etc. Here, some of the rapidly developing applications of nanotechnology is explained.

1.4.1. Electronic applications

Nanotechnology has significantly contributed to considerable advances in computing and electronics. Some of the continuously developing electronic applications include:

- Bendable, foldable, flexible, and stretchable electronic devices are reaching into different sectors and are being incorporated into a different kind of applications such as wearables, aerospace and medical applications.
- Flexible electronic devices are manufactured using semiconductor nanomembranes and are used in smartphone and e-reader display applications.

Transistors

Transistors are the fundamental switches that activate all new computing and have been manufactured smaller and smaller in size through nanotechnology.

- In ancient days, a typical transistor size is of about 130 to 250 nanometers.
- In 2014, Intel fabricated a 14 nanometer size transistor.
- In 2015, IBM manufactured the first 7 nm size transistor.
- In 2016, Lawrence Berkeley National Lab fabricated a 1 nm transistor.

Magnetic random access memory

Magnetic random access memory (MRAM) is employed to boot the computers instantly. MRAM is designed by nanometer-scale magnetic tunnel junctions and can quickly and efficiently store data during a system shutdown [13].

1.4.2. Energy applications

Nanotechnology discovers application in conventional energy sources and significantly increases alternative energy perspectives to satisfy world's emerging energy demands. Many research scientists are working to develop affordable, clean and renewable energy sources using nanotechnology.

- Nanotechnology is enhancing the efficiency of fuel formulation from crude petroleum materials via better catalysis. It is also facilitating reduced fuel usage in power plants and vehicles via higher-efficiency combustion and reduced friction.

- It is also being employed for oil and gas extraction process. For example, nanotechnology based gas-lift valves are used in seaward operations.

- Scientists are examining carbon nanotubes based membranes and scrubbers to isolate carbon dioxide from power plant exhaust.

- Scientists are fabricating wires with carbon nanotubes which will have lower resistance than the high-tension wires employed in the electric grid.

1.4.3 Nanoscale sensors

Sensors and devices fabricated with nanomaterials has the advantages of cost-effectiveness and continuous supervising of the structural integrity and performance of tunnels, bridges, parking structures, rails and pathways over time. Nanoelectronic component based sensors, communications devices and other innovative system provides an enhanced transportation infrastructure. The devices are used to help drivers to maintain vehicles lane position, to adjust travel routes and to avoid congestion [13].

1.5. REVIEW OF LITERATURE

Paulchamy et.al., [14] have reported the synthesis of graphene oxide from graphite flakes by modified Hummer's method. The X-ray diffraction (XRD) pattern showed that d-spacing value of the synthesized graphene oxide was increased from 0.3 nm to 0.8 nm, after the chemical oxidation and exfoliation. Fourier transform infrared (FT-IR) spectroscopy revealed that the synthesized product was functionalized with oxide and carboxyl functional groups. The Raman spectral analysis showed that the sample had the phase vibration of G and disorder D bands. The scanning electron microscopy (SEM) analysis of the synthesized product revealed the exfoliations of graphene oxide nanosheets.

Ning Cao et.al., [15] have reported the synthesis of graphite oxide from natural flake graphite by Hummer's method through liquid oxidization and the synthesis of reduced graphene oxide by chemical reduction of graphene oxide using ammonia aqueous solution and hydrazine hydrate. The XRD results indicated that the layer spacing of graphite oxide was longer than that of graphite. FT-IR spectroscopy showed that the product material have large amount of oxygen containing functional groups. The SEM images showed the folded morphologies of the product material. They compared the traditional chemical vapour deposition (CVD) method with the Hummer's method and reported that the graphene oxide synthesized using modified Hummer's method is cost effective and easily dispersed in water.

Deepak Kumar Gupta et.al., [16] have reported the synthesis of graphene oxide using natural graphite flake via Hummer's method. The synthesis of graphene oxide was confirmed by Raman spectral analysis with the prominent D and G band at 1392 cm^{-1} and 1592 cm^{-1} respectively. Scanning Electron Microscopy analysis of the graphene oxide indicated the layered structured ultrathin and homogeneous graphene films. Agar disc diffusion methods have been employed for the antibacterial activity of synthesized graphene oxide. The graphene oxide was tested against S. Epidermidis, E. Aerogenes, B. Subtilis and P. Aeroginosa and the zone of inhibition were found to be 12 mm, 12 mm, 9 mm and 7 mm respectively. The results showed that graphene oxide nanoparticles presented good antibacterial activity effective against common human pathogenic microorganisms.

Foo Wah Low et.al., [17] have studied the synthesis of reduced graphene oxide sheets using hydrazine solvent as a reducing agent through chemical reduction method. They have examined the effect of stirring duration at a high speed of 1200 rpm on the formation of nanoscale reduced graphene oxide sheets. The FT-IR analysis revealed the elimination of hydroxyl groups from the carbon basal plane which, was achieved after the high speed stirring for 72 hours. The distance between consecutive carbon layers (d-spacing) increased from 0.335 nm to 0.703 nm because of the introduction of oxide functional groups to carbon basal plane as examined from XRD analysis. The UV-Visible spectra recorded from the synthesized graphene oxide and reduced graphene oxide had absorbance peaks at 272 nm and 284 nm, respectively. The SEM analysis of the samples revealed the thickness of the GO and rGO sheets were 89.2 nm and 46 nm in range and revealed their sheet like structure. The silk like shaped rGO sheets were confirmed by transmission electron microscope (TEM). The I-V characteristic curves showed that the ultrathin monolayer rGO sheets could enhance the transportation of photon induced charge carriers compared to GO and graphite samples.

Jianguo Song et.al., [18] have studied the synthesis of graphene oxide (GO) films with two-dimensional structure via the modified Hummer's method. Crystal structure and presence of oxygen functional groups in the GO films were investigated by XRD and FT-IR analysis. TEM and Design For Manufacturing (DFM) analyses showed that the prepared GO sheets had single and double lamellar layer structure with the thickness of 2-3 nm. The formations of GO sheets by UV-Vis characterization were confirmed from the peaks at 380 nm. The thermo gravimetric analysis (TGA) of GO sheets at different reaction temperature ranges (100˚, 225˚ and 620˚ C) was reported. The X-ray photoelectron spectroscopy (XPS) result suggested that the GO sheet contains large numbers of functional groups on its surface, such as C-O and C=O.

Dipanwita Majumdar et.al., [19] have investigated the novel and inexpensive sonochemical approach to synthesize Beta-cyclodextrin functionalized graphene oxide (GO-CD) from aqueous solution and characterized using FT-IR, TGA, Raman and TEM analysis. FT-IR spectra of GO-CD sample showed the stretching vibration of both the GO and CD with slight peak shift in typical graphene oxide. The TGA analysis showed the percentage of cyclodextrin in the synthesized sample and was found to be 50%. They have confirmed from the thermal study that the product sample was less stable

than graphene oxide which might be due to the loss of cohesive interaction between GO sheets with β-CD during its transformation to GO-CD. Raman spectral analysis showed the ratio between D band G bands were increased from 0.957 to 0.998, which confirmed the functionalization of β-CD with GO. The TEM analysis revealed that the morphology of the synthesized sample was more crumpled than that in GO, which was invariably possible due to functionalization of GO to GO-CD. The dye adsorption property of GO-CD was evaluated against brilliant green dye and removal rate was found to be 91.21 % which was appreciably higher compared to other adsorbents.

Shanshan Wang et.al., [20] have employed the novel method for the preparation of β-cyclodextrin grafted graphene oxide. The functionalization of β-CD with GO by FT-IR spectra were confirmed from the functional groups such as oxygen, carboxyl in the range of 1000 cm^{-1} to 3500 cm^{-1}. The Raman spectra revealed the value of I_D/I_G ratio was increased from 1.43 to 1.56 due to the attachment of β-CD in the edges of GO. They have calculated the amount of β-CD grafted on the surface of GO by TGA analysis and it was found to 36.5 mg/g. Adsorption methods have been employed for the dye adsorption capacity of synthesized nanocomposites. They tested against fuchsin acid at room temperature for the different physical conditions. The removal percentage of fuchsin acid was found to be 85.2%.

Ming Chen et.al., [21] have reported the simple wet chemical strategy to synthesize reduced graphene oxide (rGO) modified with water soluble β-cyclodextrin polymer. The morphological analysis of the product sample showed that the transparent silk fabric like structure. The electrochemical sensing property of synthesized β-CD modified rGO nanocomposites were investigated against imidacloprid pesticide (IDP) using differential pulse voltammetry method. The report showed that the reduction peak current increased linearly with the concentration of IDP in linear range of 5×10^{-8} to 1.5×10^{-5} mol L^{-1} and 2×10^{-5} to 1.5×10^{-4} mol L^{-1} with detection limit of 2×10^{-8} mol L^{-1} at a signal-to-noise ratio of 3.

Yujing Guo et.al., [22] have reported the simple wet chemical strategy for the preparation of organic and inorganic cyclodextrin-graphene (CD-GNs) hybrid nanosheets. The GO-CD hybrid nanosheets have been prepared from 2.5 mg/ml aqueous solution of graphene nanosheets. The synthesized CD-GNs were characterized by UV-Vis spectroscopy, TGA, XPS, FT-IR, Raman spectroscopy, Atomic force

microscopy (AFM) and TEM analysis. The UV-Vis spectra absorption spectra of CD-GNs nanocomposite had the absorbance peak at 264 nm. It was investigated using TGA analysis that the amount of CD molecules deposited on the GNs surface ranged from 37 to 38.2 wt%.

Abolfazl Heydari et.al., [23] have employed easy in-situ polymerization route to synthesize a water-insoluble β-cyclodextrin (β-CD)/graphene oxide (GO) or reduced graphene oxide (rGO) nanocomposite hydrogels. They have used citric acid as a crosslinker to polycondense the synthesized hybrid materials. The chemical functionalization of graphene oxide with cyclodextrin polymer (CDP) were confirmed by Raman analysis and the I_D/I_G ratio values of CDP-CT/GO was 1.8, which was higher than in comparison with GO (1.65). The SEM analysis revealed the parallelogram shapes of CD particles formed on the stacked layers of graphene oxide. The energy dispersive X-ray (EDAX) measurements showed that the presence of carbon in the CDP-CT/GO has been decreased and the amount of oxygen in comparison with CDP-CT has been increased, which confirmed the existence of GO nanofiller in the synthesized nanocomposites. The TGA results showed the enhancement in the thermal stability have been due to the interaction between the polymer matrix and GO or rGO nanosheet, which could act as barriers, maximizing the heat insulation and minimizing the permeability of volatile degradation products to the material. Cyclic voltammetry (CV) and Difference Pulse Voltammetry (DPV) methods have been employed to study the electrochemical activity of synthesized nanocomposites. These were tested against dopamine, tyrosine and uric acid. The best electrochemical detection property was obtained for the CDP-CT/rGO nanocomposites related to CDP-CT/GO, which might be probably due to the restoration of graphitic networks after the reduction.

John H. Xin et.al., [24] have reported the one pot functionalization and reduction process for the synthesis of functionalized graphene using the bio-based β-cyclodextrin as a covalent modifier (CD-G). The UV-Vis spectra recorded from the reaction medium showed the absorption spectra of CD-G formed have absorbance peak at 269 nm. The FT-IR spectrum of CD-G showed that the β-CD molecules were not physically adsorbed but chemically grafted on the CD-G surfaces. The surface morphology analysis of CD-G revealed the uneven and rough surface topology of the nanocomposites, which could be attributed to the β-CD molecules incorporating on the

CD-G surfaces. They have fabricated the fluorescence probe using CD-G and RhB molecules through facile and economical solution mixing method. The fluorescence probe was analyzed for their quenching activity against a wide range of water-soluble and insoluble organic solvents. The result showed the highest sensitivity to tetrahydrofuran (THF), with the limit of detection of about 1.7 μg/mL.

Mild and novel preparation tactics based on electrochemical techniques for the fabrication of electro-deposited graphene (E-GR) and polymerized β-cyclodextrin (P-βCD) nanocomposite film have been reported by **Yaping Ding et.al.,** [25]. The scanning electron microscope and transmission electron microscope showed sheet-like, glossy and crimple shape graphene oxide sheets. The D/G band intensity ratios of synthesized product were calculated to be 1.4 and 1.2 using Raman spectroscopy. The electrochemical response of E-GR/P-βCD/GCE to quercetin was investigated using difference pulse voltammetry (DPV) techniques showed that the produced sensor greatly facilitated the oxidation of quercetin with the detection limit of 0.001 mM.

Song-Jie Qiao et.al., [26] have studied the functionalization and reduction of graphene oxide by a 4-hydrazinobenzenesulfonic acid (HBS), with a one-step and environmentally friendly process. The interlayer space of HBS-rGO was increased to 1.478 nm from 0.751 nm as found by XRD analysis. The SEM images showed that as a result of longer interlayer space and weaker vanderwaals force, the synthesized HBS-rGO was not aggregated. The ratio of I_D/I_G obtained by Raman analysis of HBS-rGO sample was 0.29, which was much less than that of graphene oxide (GO). The XPS result showed that the oxygen content was dropped from 17.19 % to 7.23 % for HBS-rGO, confirmed the successful reduction of graphene oxide by HBS. The aqueous dispersibility of graphene was improved because of the functionalization from 0.58 mg/mL to 13.49 mg/mL.

The synthesis of silver nanoparticles (Ag) in an aqueous suspension of graphene oxide via chemical reduction method has been reported by **Manash R. Das et.al.,** [27]. The experiment was conducted for four different concentrations of (1 mM, 2 mM, 4 mM and 8 mM) silver nitrate. The UV-Visible spectra of nanoparticles showed a red shift with increasing concentrations. TEM images of Ag nanoparticles showed the wide distribution of spherical shaped nanoparticles ranging in the diameter of 5-25 nm. Agar disc diffusion methods have been employed for the antibacterial activity of synthesized

nanoparticles. They tested against Echeria coli (E. Coli) and Pseudomonas aeruginosa (P. Aeruginosa) for different concentration of the silver nitrate. The best inhibition zone was found against P. Aeruginosa pathogens for the 4 mM concentration of silver nitrate.

A simple wet-chemical pathway has been demonstrated for the synthesis of silver nanoparticle conjugated reduced graphene oxide nanosheets (Ag/rGO) by **Soumen Dutta et.al.,** [28]. The reduction of silver nitrate into silver nanoparticles by dimethylformamide (DMF) was completed after 20 hours. The formation of silver nanoparticles/reduced graphene oxide was confirmed by Surface Plasmon Resonance (SPR) at 254 nm and 411 nm using UV-Visible spectrophotometer. TEM analysis confirmed the spherical shaped silver nanoparticles with the particle size of 20-40 nm. The XRD analysis showed that the silver nanoparticles on the rGO sheets were crystalline in nature and had face centred cubic geometry. The presence of oxygen functionalities and skeletal vibrations in the synthesized Ag/rGO samples were investigated by FT-IR analysis. Raman spectra showed that the I_D/I_G value increases from 0.94 to 1.08 during GO to Ag/rGO conversion, which indicated the formation of new and isolated smaller graphitic domains. The synthesized Ag/rGO nanocomposites were found to be highly sensitive for the adsorption of uranyl ions with the detection limit as low as 10 nM.

The glucose and poly (N-vinyl-2-pyrrolidone) (PVP) have been used for their simultaneous reduction synthesis of graphene decorated with various concentration (25%, 40% and 60%) of silver nanoparticles by **Zhong-Zhen Yu et.al.,** [29]. UV-visible spectroscopy has been used to monitor the quantitative formation of silver nanoparticles. FT-IR spectral analysis showed that the peaks corresponding to the oxygen containing groups gradually decreased, which might be due to the reduction and decoration of silver nanoparticles on the GO sheets. The morphological analysis showed that the quantity of silver nanoparticles on the surface of GO sheets was found to be higher for lower concentration of silver. The signals of RhB were stronger for lower concentration than those of higher concentration of silver has been investigated by Raman spectral analysis.

Khaled Habiba et.al., [30] have investigated the synthesis of silver nanoparticles decorated with graphene quantum dots (Ag-GQDs) using pulsed laser synthesis method. The High resolution TEM (HR-TEM) analysis of the nanocomposites

showed a diameter of 10 nm with an interplanar spacing of 0.145 nm that matches with the (220) plane of silver. The antibacterial activity of Ag-GQDs was evaluated and compared to that of bare GQDs and commercial silver nanoparticles (Ag-NPs) against both gram-negative and gram-positive bacteria, using Pseudomonas aeruginosa and Staphylococcus aureus as model bacteria, respectively. The zone of inhibition for gram-negative and gram-positive bacteria's was reported to be 10 to 15 mm.

The synthesis of graphene oxide (GO)-silver nanocomposites and its antibacterial activity against relevant microorganisms in medicines have been reported by **Ana Carolina Mazarin de Moraes et.al.,** [31]. The GO sheets were functionalized with silver nanoparticles (AgNPs) using a modified Turkevich method. Graphene oxide-silver nanocomposites were characterized using UV is absorption spectroscopy, FTIR, XRD, TGA, XPS, and TEM analysis. UV-visible spectrophotometer analysis showed the absorbance peak at about 263 nm and 410 nm indicating the attachment of silver nanoparticles to the GO surface. The attachment of AgNPs to the GO sheet surface has been evaluated by XRD patterns and the results showed that the crystalline planes of face-centered cubic silver nanoparticles have been attached to GO surfaces. The TGA of synthesized nanomaterials displayed the mass ratio proportion of Ag:GO was approximately 1:1. The spherical-like AgNPs with the average size of about 9.4 nm were well-dispersed throughout the GO sheets and were exclusively investigated by TEM. The GO-Ag nanocomposite exhibited antibacterial activity against bacteria commonly found in hospital environments, such as E. coli, E. faecalis, A. Baumannii and the antibiotic-resistant MRSA.

The evaporation induced self assembly and photo induced self assembly synthesis of mesoporous Bi-S-TiO_2/β-CD and its photocatalytic activity have been reported by **Guoqi Feng et.al.,** [32]. The band gap value recorded by UV-Vis spectroscopy for the mesoporous Bi-S-TiO_2/β-CD wire was found to be 2.67 eV. The XRD result revealed that the anatase phase of TiO_2 in the mesoporous Bi-S-TiO_2/β-CD wires conserved their anatase crystal features. The SEM analysis revealed that the size of the TiO_2 particles were small and independent. The HR-TEM analysis showed that the average particle size of about 10 nm in range and revealed their crystalline nature. The nanowires at the concentration of 1.5% of Bi showed complete photocatalytic activity against dinitrotoluene (DNT) and the degradation ability were found to be

95.5%. The study reported that the synthesized mesoporous Bi-S-TiO_2/β-CD wire were more efficient in photocatalytic degradation product.

Highly sensitive and selective electrochemical catechol (CT) sensor based on gold nanoparticles (AuNPs) decorated on graphene oxide @ polydopamine (GO@PDA) composite modified glassy carbon electrode was demonstrated by **Selvakumar Palanisamy et.al.,** [33]. The formation of gold nanoparticles on GO@PDA was confirmed by SEM analysis, with the average diameter of about 52 nm. The FT-IR spectra showed the peaks for GO with the additional characteristic peak at 1366 which was due to the typical vibration of phenolic C-O-H bending in PDA. The good electrochemical activity towards the detection of catechol was tested and the nanocomposite modified electrode showed an enhanced oxidation peak current response and low oxidation potential for the detection of CT, which was found to be linear for the concentration ranging from 0.3 to 67.55 μM, with the detection limit of 0.015 μM. The sensitivity of the produced sensor was estimated as 4.66 ± 0.15 μA $\mu M^{-1}cm^{-2}$.

Self-assembly of positively charged gold nanoparticles on negatively charged 1-pyrene butyric acid functionalized graphene (PFG) sheets for the ultrasensitive detection of uric acid have been investigated by **Wenjing Hong et.al.,** [34]. TEM study revealed that gold nanoparticles with the average size of 2 to 6 nm were extensively assembled on PFG sheets upon strong electrostatic interaction between both the components.

A novel electrochemical sensor for para-nitrophenol (p-NP) was constructed with graphene-Au composite containing 10 % Au (G-Au 10 %) have been investigated by **Wenbei Zhang et.al.,** [35]. The experiment was carried out for the different concentrations of gold precursor (5 %, 10 % and 20 %). X-ray diffraction spectra of G-Au nanocomposites formed in the reaction media had shown diffraction peaks corresponding to the fcc structure of gold nanoparticles with the average crystallite size of the gold nanoparticles of about 12.1 nm. TEM images revealed that the G-Au nanocomposites formed with 10 % of $HAuCl_4$ demonstrated a relatively higher Au density on graphene sheet without aggregation; hence it could be a more suitable catalyst in constructing electrochemical sensors. Amperometric detection of p-NP at G-

Au 10 % modified GCE electrode displayed a wide range of linear detection 0.47-10.75 mM with detection limit of 0.47l M and a high sensitivity of 52.85l A/mM.

Ping Li et.al., [36] have investigated the enhancement of interfacial interaction between poly vinyl chloride (PVC) and reduced graphene oxide (rGO) by decorating rGO with zinc oxide (ZnO) nanoparticles. The synthesis of rGO loaded with ZnO nanoparticles (rGO-ZnO) was achieved through one-pot chemical route. XRD results of the rGO/ZnO nanocomposite confirmed the successful formation of hexagonal ZnO during the hydrothermal process. SEM and TEM images of rGO/ZnO nanocomposites showed nanorods with an average width of 100 nm and an average length of 300 nm, which were uniformly distributed on the surface of rGO sheets. The rGO/ZnO hybrid nanoparticles exhibited superior capacitive behaviour and high interfacial interaction with PVC chains, compared to physical blended GNPs/ZnO nanoparticles.

Kuo-Yuan Hwa et., [37] have reported the preparation of zinc oxide nanoparticles incorporated graphene-carbon nanotubes hybrid (GR-CNT-ZnO) through a simple, one-pot method. The synthesized GR-CNT-ZnO composite was applied to fabricate an enzyme based glucose biosensor. The SEM image of the GR-CNT-ZnO nanocomposites showed that the GR-CNT sheets were decorated with numerous ZnO nanoparticles in the size that ranged between 50-80 nm. TEM analysis confirmed the incorporation of ZnO nanoparticles within the GR-CNT nanosheets. The proposed sensor had a wide range of linear detection from10 μM to 6.5 mM of glucose with a limit of detection (LOD) of 4.5 μM.

Murugan Saranya et.al., [38] have investigated the facile solvothermal approach for the synthesis of well crystalline graphene-zinc oxide nanocomposites. XRD results showed that the crystalline planes were indexed to the wurtzite structure of ZnO particles with an average ZnO crystallite size of 14 nm. The formation of ZnO-GN was confirmed by surface plasmon resonance as determined by UV-Vis spectra at 398 nm. The particle size of ZnO nanoparticles were reported to be 30 nm using TEM. These nanocomposites showed a good capacitive behaviour with a specific capacitance of 122.4 F/g as compared to graphene oxide (2.13 F/g) and rGO (102.5 F/g) at 5 mV/s scan rate.

Xuan Zhang et.al., [39] have reported the one pot spontaneous reduction method for the synthesis of reduced graphene oxide-zinc oxide (RGO–ZnO) composite at room temperature. The formation of RGO-ZnO nanocomposites were characterized using XRD, TEM and SEM analysis. SEM analysis showed that the ZnO nanoparticles with the average size around 300 nm and were well distributed and wrapped by rGO sheets. The synthesized nanocomposites were tested against the detection of ascorbic acid (AA), dopamine (DA) and uric acid (UA). The liner relationships between current intensities and concentrations were found to be 50-2350 μM, 1-70 μM and 3-330 μM, with detection limits of 3.71 μM, 0.33 μM and 1.08 μM for AA, UA and DA, respectively.

A facile graphene-copper nanocomposite was synthesized and investigated by **Qiwen Chen et.al.,** [40]. The morphological studies revealed that the copper nanoparticles with a diameter of 20.8 nm were deposited on the surface of graphene nanosheets to produce a highly interconnected hybrid network. The electro-analytical performance of the synthesized graphene-copper nanocomposite was studied by sensing five different carbohydrates and the sensitivity was determined to be 85.96 nA/mM for mannitol, 52.63 nA/mM for sucrose, 50.88 nA/mM for lactose, 63.16 nA/mM for glucose and 45.61 nA/mM for fructose respectively.

Wei Wu et.al., [41] have investigated the facile one-pot reduction method for the synthesis of graphene-copper (GNS-Cu) nanocomposite. The morphological analysis revealed that the copper nanoparticles with a diameter of 20 nm were homogeneously deposited on the surface of graphene sheets. The antifriction behaviour of the base oil when added with synthesized GNS-Cu nanocomposite was investigated and showed the siginificant antifriction behaviour.

Jaewon Hwang et.al., [42] have reported the synthesis of graphene-copper nanocomposites using molecular level mixing process. The AFM analysis showed that the synthesized nanocomposites were not agglomerated and the thickness of the GO sheet was found to be 1 nm. The SEM analysis revealed that the smooth surface of graphene oxide nanosheets was uniformly covered with copper oxide nanoparticles. The elastic modulus and the yield strength of the synthesized RGO/Cu nanocomposite were found to be 131 GPa and 284 MPa, respectively.

Ting Hu et.al., [43] have reported the one step in-situ synthesis procedure for ZnO@reduced graphene oxide-poly (N-vinylpyrrolidone) nanocomposite for enhancing the performance of solar cells. The XRD pattern showed that the peak corresponding to GO at 10˚ was disappeared and replaced by new broad diffraction peak around 20˚ to 30˚, which indicated the disordered stacking of graphene nanosheets in rGO-PVP. The intensity ratio of the D and G bands in the Raman spectra for GO was found to be increased from 1.07 to 1.16 for rGO-PVP, which confirmed an increase in the number of smaller in-plane sp^2 domains during the reduction of GO. The inclusion of PVP in the synthesized rGO-PVP was also confirmed from TGA analysis by a significant weight loss in the temperature range from 300˚ to 500˚ C. The photovoltaic study confirmed that the incorporation of ZnO@RGO-PVP nanocomposite as cathode buffer layer improved the PCE value of the device to 7.5 %.

Facile synthesis of various zinc oxide (ZnO) nanostructures on reduced graphene oxide (RGO) nanosheets by an in situ hydrothermal reaction process was investigated by **Junwei Ding et.al.,** [44]. The SEM images of the synthesized rGO-ZnO nanocomposite showed that the unique folded morphology of rGO nanosheets were uniformly covered with the microspindle ZnO nanostructures for the mass ratio of 4.4:1. The as prepared ZnO-rGO nanocomposites with various nanostructures were immobilized onto the glassy carbon electrode surface and employed to fabricate an electrochemical hydrazine sensors. The electrochemical studies indicated that the ZnO-rGO nanocomposites synthesized with the mass ratio of 4.4:1 provided the best sensor behaviour. The fabricated hydrazine sensor exhibited a good amperometric response with a linear range of detection from 1.0 mM to 33.5 mM and a detection limit of 0.8 mM.

1.6. MATERIALS AND METHODS

The chemicals required for the synthesis of metal (Ag, Au) / metal oxide (ZnO, CuO) nanoparticles embellished β-cyclodextrin functionalized reduced graphene oxide nanocomposite are purchased from Himedia Pvt. Ltd. and are listed as:

- **Graphite powder (<20 µm, synthetic)**
- **β-Cyclodextrin polymer**

- **Silver nitrate ($AgNO_3$)**
- **Gold (III) chloride trihydrate ($HAuCl_4.3H_2O$)**
- **Zinc acetate dihydrate ($C_6H_4O_4Zn.2H_2O$)**
- **Copper II acetate monohydrate ($CH_3COOC_4.H_2O$)**
- **Sodium borohydride ($NaBH_4$)**

1.6.1. Graphite

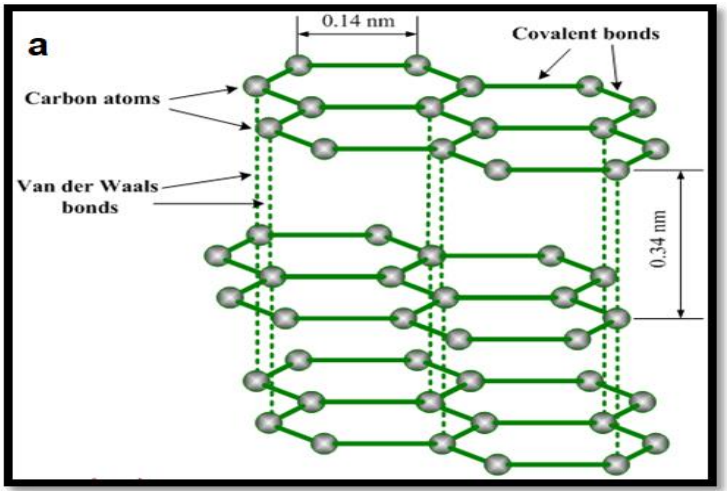

Figure.1.3. Structure of graphite

Graphite is known to be the most stable form of carbon allotropes under some standard conditions. The name graphite derived from the Greek word graphein. The appearance of the material is usually greyish-black colour. Graphite has the properties of both the metals and non metals. It also has the unique properties such as high thermal conductivity, flexibility but not elastic and have high electrical conductivity due to its excellent crystal structure. Graphite has a layered structure as shown in the Figure.1.3, in which the carbon atoms are arranged in a honeycomb lattice with separation of 0.142 nm and the distance between the planes are found to be 0.335 nm. The layers are weakly bonded together by vanderwaals forces but the atoms in the layers are covalently bonded [45].

1.6.2. Graphite oxide

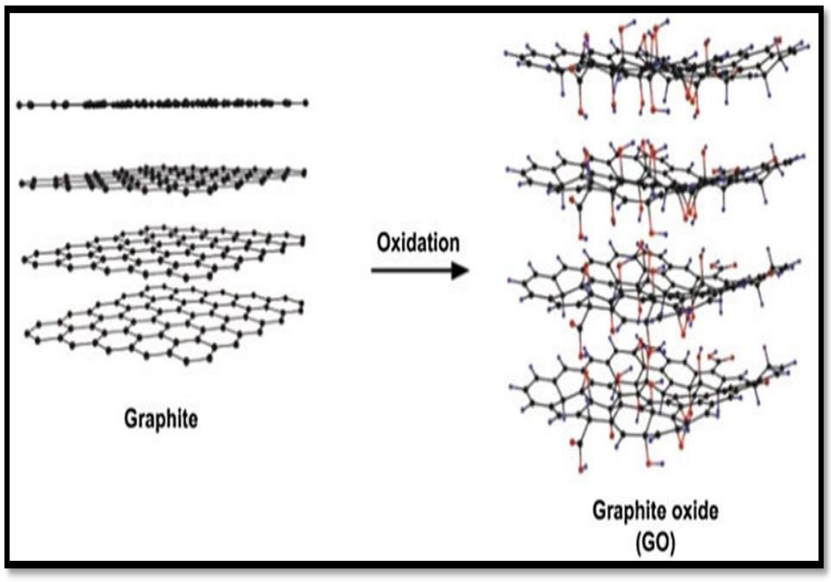

Figure.1.4. Structure of graphite oxide

Graphite oxide is commonly a solid material and is in yellowish colour. It has a layered structure like that of graphite as shown in the Figure.1.4, but the plane of carbon atoms in the graphite oxide is densely decorated by oxygen-containing functional groups. These functional groups not only increases the interlayer distance but also make the graphite oxide as hydrophilic. These oxygen functionalized layers could be peeled off in aqueous medium under ultrasonication process. The exfoliated graphite oxide sheets contain one or a few layers of carbon atoms like graphene and these exfoliated sheets are named as graphene oxide (GO) [46].

1.6.3. Graphene oxide

Graphene oxide is obtained by the oxidation of graphite oxide, which is modest and abundant [47]. The schematic representation of structure of graphene oxide is shown in the Figure.1.5

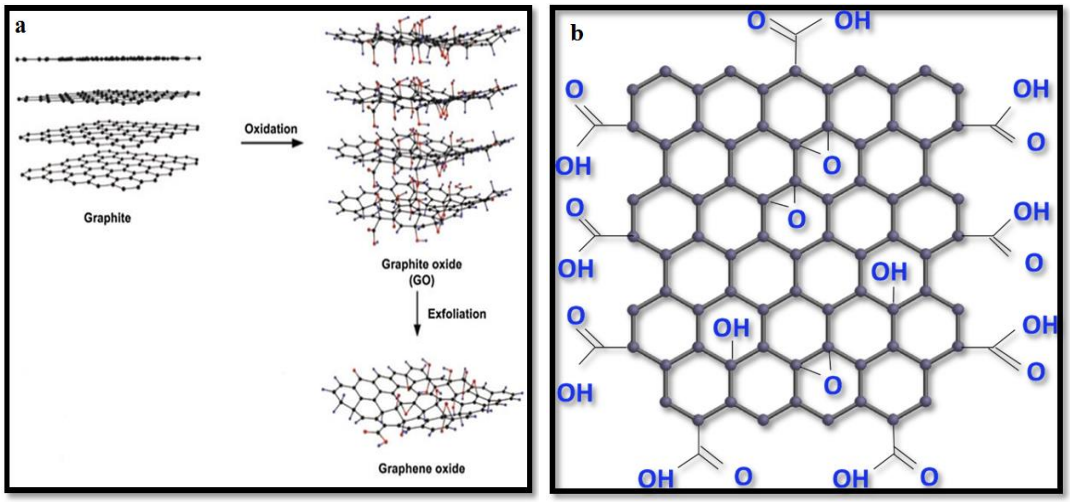

Figure.1.5. (a) and (b) structures of graphene oxide

It is a single atomic thick layered structured material, containing carbon, hydrogen and various oxygen containing functional groups such as hydroxyl, carboxyl, carbonyl and epoxy groups. These oxygenated functional groups are embedded on both the edge and basal plane of the graphene oxide nanosheets [48].

1.6.3.1. Synthesis of graphene oxide

The various synthesis method of graphene oxide is shown in the Figure.1.6. Chemical synthesis method allows the mass production of graphene oxide nanosheets which cannot be accomplished by the other synthesis methods such as chemical vapour deposition (CVD), mechanical exfoliation, liquid phase exfoliation of graphite and epitaxial growth. This method of graphene oxide consists of oxidation and reduction steps. In a typical synthesis method, graphite is oxidized to graphite oxide (GO) with the help of oxidizing agents such as $KMnO_4$, H_2SO_4, HNO_3, H_3PO_4 and $KClO_3$ [49]. The oxidation of graphite materials leads to the increase in the interlayer spacing of graphene oxide nanosheets which may be due to the inclusion of oxygenated functional groups on the layers. As the oxidation degree is excellent, the possibility to produce high quality graphene oxide is also higher. The degree of oxidation is enhanced from Brodie's method to Staudenmaier's, Hummer's, modified Hummer's and currently Tour's method.

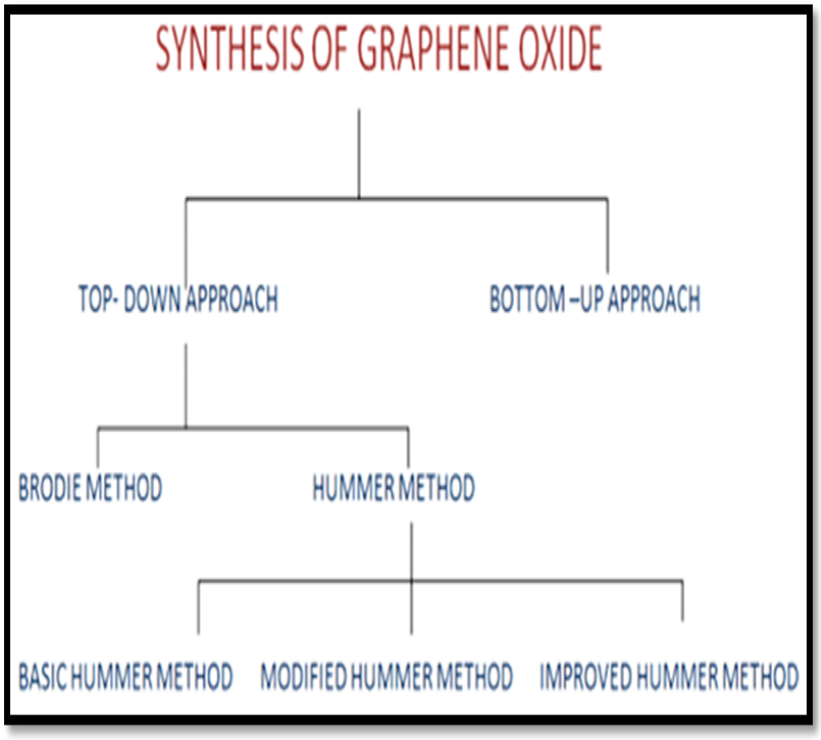

Figure.1.6. Synthesis methods of graphene oxide

In 1859 the British Chemist B.C. Brodie have examined the graphite structure for the synthesis of graphene oxide using graphite, potassium chlorate ($KClO_3$) and fuming nitric acid (HNO_3) [50]. In 1898, L. Staudenmaier has made a minor change to the Brodie's method to enhance the oxidation mechanism of graphite by the addition of concentrated sulfuric acid (H_2SO_4), potassium chlorate ($KClO_3$) and fuming nitric acid (HNO_3). In 1958, the chemist Hummer's has introduced an alternative oxidation technique for the synthesis of graphene oxide, which is the most widely used technique nowadays [51].

Modified Hummer's method

Modified Hummer's method of synthesis corresponds to both the exfoliation and oxidation of graphite sheets due to the heat treatment of reaction solution. The stepwise synthesis technique is given as follows [52]: Graphite flakes of about 2 g and sodium nitrate of about 2 g are mixed in 90 mL of concentrated H_2SO_4 (98%) in a 1000 ml of beaker and kept under ice bath at 0-5°C with continuous stirring. The reaction mixture is then stirred for 4 hours under ice bath condition and potassium permanganate of about 12 g is added to the reaction suspension very slowly. The rate of addition is carefully

governed to keep the solution temperature lower than 15˚C. The reaction mixture is then diluted with the addition of 184 ml of deionised water and stirred for 2 hrs. The ice bath is then removed, and the reaction mixture is stirred at 35˚C for 2 hrs. Then, the above reaction mixture is kept in a reflux system at 98˚C for 10-15 minutes and then the reaction temperature is changed to 35˚C. The reaction solution is then treated with 40 ml of H_2O_2 by which the colour of the mixture changes to yellow. 200 mL of distilled water is taken in two separate beakers and equal amount of reaction suspension is synthesized and stirred for 1 hour. It is then kept undisturbed for 3-4 hours, where the nanoparticles settles at the bottom and remaining water is poured off. The resulting reaction mixture is washed thoroughly by centrifugation using 10 % HCl and then with distilled water. The gel like material formed is dried at 60˚C for more than 6 hours [52].

1.6.3.2. Structure of graphene oxide

The structure of graphene oxide is highly depend on the oxidation conditions, the graphite precursor material employed and workup treatments. Based on these conditions, various structural models of graphene oxides have been proposed by many scientists and are as shown in Figure.1.7.

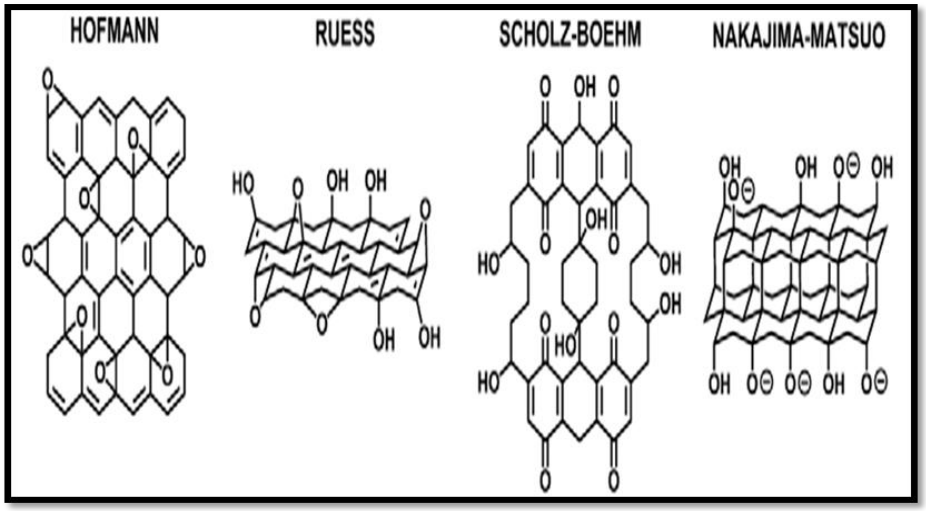

(a)

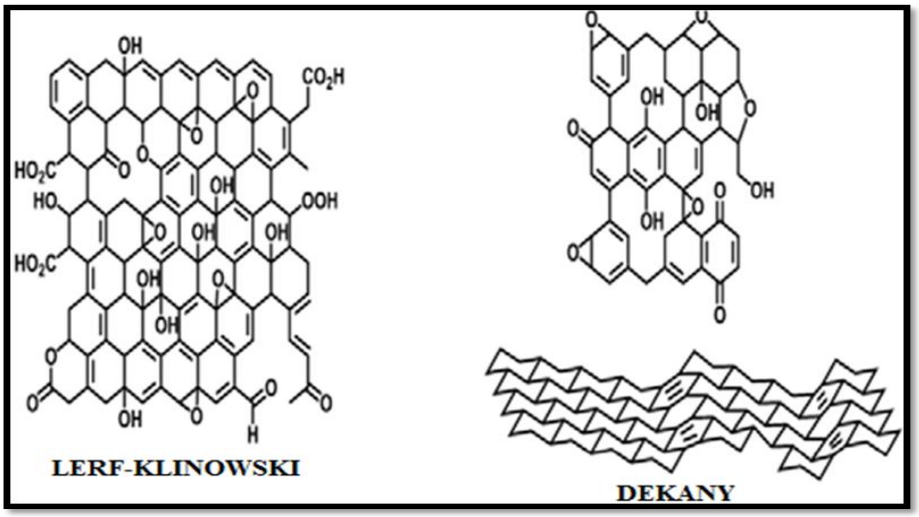

(b)

Figure.1.7. (a) Hofmann, Ruess, Scholz, Nakajima (b) Lerf, Dekany structures of Graphene Oxide

Hofmann and co-workers have proposed a model of graphene oxide structure that contains epoxy groups and these groups are diffused across the basal planes of graphite with a net molecular form of C_2O [53-54]. In 1946, the Hofmann structural model is reshaped by Ruess, who included the hydroxyl groups into the basal planes of graphene oxide. Further, Ruess modified sp^2 hybridized basal plane structure into sp^3 hybridized structure [53]. Scholz-Boehm, Nakajima and Matsuo also proposed an esteemed structural model to realize the chemical structure of graphene oxide. According to Scholz and Boehm's model, the graphene oxide structure contains regular quinoidal species in a wrinkled backbone, where they have entirely removed the ether and epoxide groups from the carbon structure [53] [55].

The Lerf–Klinowski structural model has been the most acknowledged and widely accepted model which depends on a non-stoichiometric and amorphous structure model. Their model has explained two different regions:

- First one is conventionally aromatic regions with unoxidized benzene rings.
- The second region is found to be with the aliphatic six member rings [55].

The approximate size of the regions is calculated by using the degree of oxidation of graphene oxide. In the Lerf-Klinowski model, the basal plane of graphene oxide is enriched with epoxide and hydroxyl, which are relative to one another and the layers are bonded with C-COOH and C-OH groups. Only the hydroxyl groups attached carbon atoms are in distorted tetrahedral configuration and thereby introducing some wrinkling of the layers. In this model, the functional groups are attached, both above and below the carbon layers forming a negatively charged layer of oxygen atoms that avoid nucleophilic [55]. Their structural model further indicated that the water molecules are strongly attached to the basal plane of graphene oxide through hydrogen bonds [55-56].

Dekany has re-established and updated the Ruess and Scholz-Boehm structural models based on their Diffuse Reflectance Infrared Fourier Transform (DRIFT) and FT-IR spectroscopic studies [57]. They have found from the IR study that the characteristic band at 1714 cm^{-1} may be attributed to the ketones and/or quinines functional groups of graphene oxide. They have incorporated phenolic groups into the bulk graphene oxide structure by which the planar acidity can be explained. This model also displays a carbon skeleton containing two distinct domains trans-linked cyclohexane chairs connected with ethers, tertiary alcohols and ribbons of flat hexagons of keto/quinoidal functional groups. A slight bending between the boundaries of these regions can be the desirable basis for the wrinkled structure of graphene oxide [58]. Hence, the determination of the precise chemical structure of graphene oxide has been a challenge due to its non-stoichiometric chemical formation.

1.6.3.3 Properties of graphene oxide

Graphene oxide can be employed for the various applications in the field of semiconductors, electronics, sensors, gas absorbers, fuel cells, optic devices, solar cells and composites due to their phenomenal properties such as electrical, mechanical and thermal properties. Graphene oxide is dispersible in aqueous medium and it has the following outstanding characteristics:

- Graphene oxide is dreadfully hydrophilic in nature and can produce stable aqueous colloids to aid the accumulation of macroscopic structures by facile and cheap solution methods [58].

- The densely decorated graphene oxide sheets contain tetrahedrally bonded sp^3 hybridized carbon atoms, which are dislocated hardly below or above the graphene planes [59].

- Graphene oxide sheets are atomically wrinkled because of the structural dislocation and the existence of covalently bonded oxygenated functional groups in the graphene oxide sheets [60-61]

- Graphene oxide surface is highly deficient, possibly due to the presence of oxygenated functional groups, and other areas of graphene oxide nanosheets are almost perfect [62-64].

- Graphene oxide nanosheets has the graphene like hexagonal lattice structure despite with some disorders (i.e., the carbon atoms bonded to functional groups are slightly dislocated) [65].

Electrical Properties

Graphene oxide sheets are conventionally insulating and exhibits a sheet resistance (R_s) values of about 10^{12} Ω/sq or above due to the high density of electronegative oxygen atoms bonded to carbon atoms and the existence of sp^3 hybridized carbon array [66-67]. The chemical or thermal reduction of graphene oxide can make graphene oxide electrically conductive. The thermal treatment of graphene oxide decomposes the presence of oxygen functional groups and restores the sp^2 carbon array which leads to increase in the electrical conductivity [66] [68].

Mechanical Properties

Young's modulus of graphene oxide with the thickness of about 0.7 nm is found to be 207±23.4 GPa. The functionalization of oxygen containing functional groups modifies the ideal 2D structure of graphene oxide, which leads to decrease in the mechanical strength of graphene oxide nanosheets [69]. The Young's modulus of the value of graphene oxide is highly dependent on the molecular structure and degree of functionalization of the functional groups. The modification in the chemical structure with the existence of functional groups cause the graphene oxide sheets to become unstable and consequently degrade the elastic properties of graphene oxide nanosheets [70].

1.6.4. Reduced graphene oxide

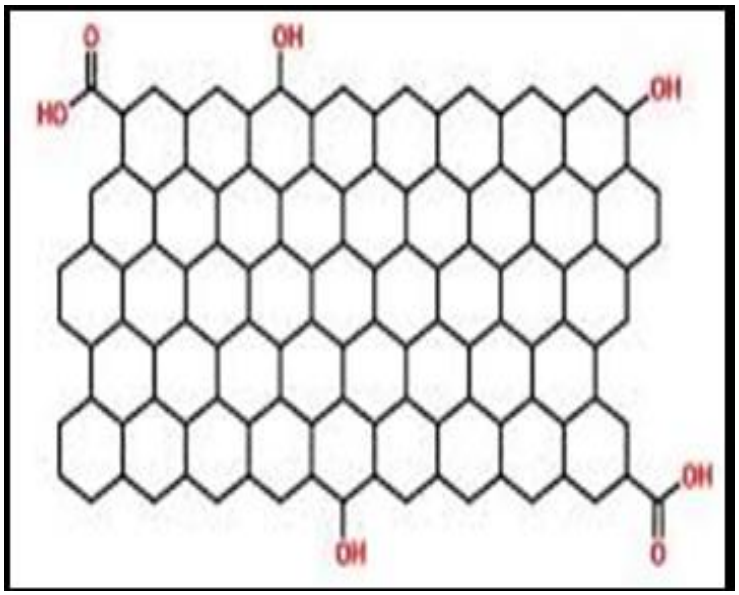

Figure.1.8. Structure of reduced graphene oxide

The reduced graphene oxide (rGO) sheets are typically considered as a one type of chemically derived graphene and are known as reduced graphene oxide. Some other names of reduced graphene oxides are chemically modified graphene, functionalized graphene, chemically converted graphene and reduced graphene [71]. The reduced graphene sheet contains only trigonally bonded sp^2 carbon atoms and is perfectly flat [72] and as shown in the Figure.1.8.

1.6.4.1. Synthesis of reduced graphene oxide

Reduced graphene oxide provides a good solution for the large-scale applications of graphene oxide such as energy storage and sensors. The reduced graphene oxide is easier to synthesize in large quantities than single-layer or few-layers of graphene. The quality of synthesized reduced graphene is well suited for the bulk material applications. The reduction of graphene oxide can be accomplished in a number of ways such as thermal, chemical and electrochemical methods [73]. The techniques which are capable of manufacturing the high quality graphene sheets tend to be more complicate. The various methods used to reduce graphene oxide are as follows:

The chemical reduction of graphene oxide is only a scalable technique to produce reduced graphene oxide. However, the reduced graphene oxide synthesized by

this technique often has low grade electrical conductivity and surface area. On the other hand, thermal reduction of graphene oxide at above 1000˚C produces a high surface area. However, this method has a major disadvantage: (i.e) the chemical structure of the reduced graphene oxide sheets are damaged by the heating mechanism, resulting in remarkable mass loss, and potentially reducing the mechanical strength of the reduced graphene oxide.

Hence, the electrochemical synthesis of reduced graphene oxide is preferred as a commercial method for the synthesis of rGO. This method of synthesis of reduced graphene oxide has the structure identical to pristine graphene. In this method, substrates like indium tin oxide or glass are coated with a thin layer of reduced graphene oxide. This technique produces a very high quality of reduced graphene oxide sheets and employs basal harmful chemicals. However, this method is challenging to scale up due to the deposition of large quantities of graphene oxide on substrates. The other available methods for the synthesis of reduced graphene oxide are as follows:

- Reduction of graphene oxide with hydrazine hydrates at the temperature of 100˚C for 24 hours.
- Exposure to hydrogen plasma on the surface of graphene oxide for several seconds.
- Transmission of powerful pulsed light from xenon flashtubes through graphene oxide.
- Heat treatment of graphene oxide with urea as a reduction agent.
- Straight heating of graphene oxide in a furnace to very high temperatures [73].

1.6.4.2. Properties of Reduced Graphene Oxide

The physico-chemical properties of reduced graphene oxide are given in Table 1.1

Table.1.1. Physicochemical properties of Reduced Graphene Oxide [45]

Properties	Nature
Form	Powder
Colour	Black
Sheet dimension	Variable
Odour	Odourless
Solubility	Insoluble
Dispersability	Dimethyl sulfoxide (DMSO), N-Methyl-2- (NMP), Dimethylformamide (DMF)
Density	1.91 g/cm^3
Humidity	3.7 - 4.2%
Electrical Conductivity	666,7 S/m
BET surface area	422.69 – 499.85 m^2/g

1.7. FUNCTIONALIZATION OF GRAPHENE

The synthesis and applications of graphene based nanomaterials are having huge interests due to their exotic properties such as electronic, magnetic, optical, mechanical and thermal properties. In comparison with pure graphene materials, functionalized graphene or membranes can bring remarkable advantages attributed to their specific functionality, hybrid structure and enriched physicochemical properties. Surface functionalization can modify pristine graphene into a soluble and chemically sensitive material, thus enabling its role in sensor technologies [74-77].

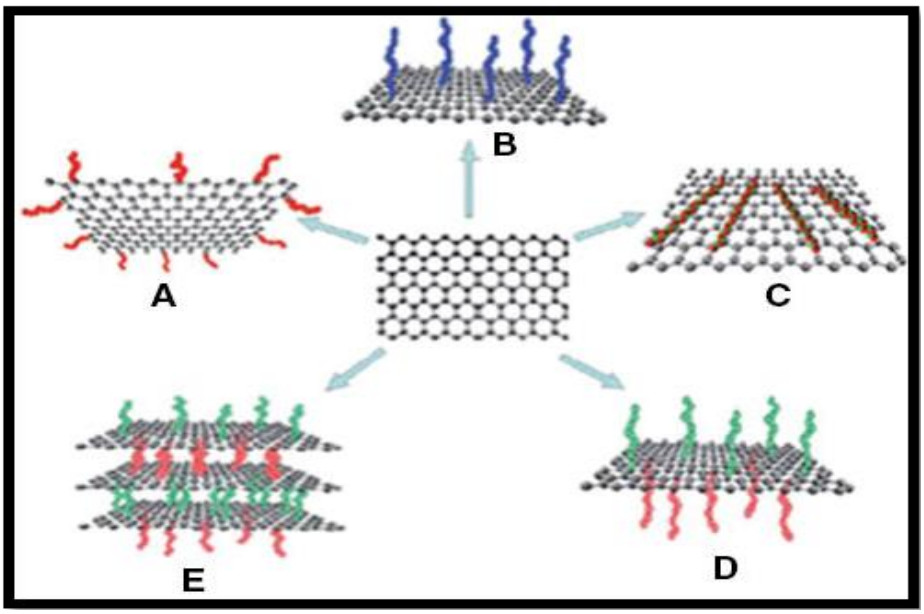

Figure.1.9. Functionalization possibilities of graphene (a) Edge (b) Basal-plane (c) Non covalent adsorption on basel plane (d) Asymmetric (e) Self assembly

Generally, graphene can able to functionalize with the various chemical components such as metals, metal oxides, polymers matrices and supramolecular units, via various techniques and are shown in the Figure.1.9. The two methods are widely used to functionalize graphene with other materials:

- The covalent functionalization through the implanting of molecules onto the sp^2 carbon atoms of the π-conjugated skeleton [78].
- The non-covalent functionalization of graphene based on the adsorption of surfactants or polycyclic aromatic compounds through the hydrophobic interactions and π-stacking on the carbon network [79].

The report outlines the functionalization of graphene materials with metallic nanostructures, metal nanocompounds and polymers, which are used for electrochemical-sensing applications.

1.7.1. Metallic nanostructures

Nanostructured metals have fascinating interests from the scientific society, because of its unique properties and multidisciplinary applications [80-81]. The number of studies has revealed that the functionalization of graphene nanosheets with the

metallic nanstructured materials enhances the synergistic effects and cooperation between nanostructured metals such as platinum (Pt) nanoparticles [82], gold (Au) nanoparticles [83], silver (Ag) nanoparticles [84] and Au/Pt core-shell nanoparticles etc. The functionalization of graphene sheets with metallic nanostructure materials increases the surface plasmon signal and electrical properties of the nanostructure graphene sheets. The functionalization of metal nanomaterials with the graphene nanosheets is done by using various physical and chemical methods. In the present study, metal nanoparticles are incorporated onto the surface of graphene nanosheets though physical loading (adsorption) method and the functionalization is found to be non-covalent.

In the metallic nanostructured materials functionalized graphene sheets; the metal nanoparticles have not activated the π-π electronic transitions in the aromatic carbon-carbon of graphene nanosheets, but have been activated by the electrostatic repulsion between the de-protonated carboxylic groups at the edge of graphene nanosheets. The electronic environment of the metal nanoparticles is modulated by its own negatively charged atoms, causing the enhancement in the electro chemical properties such as electrode kinetics and a cyclic voltammetric response. This enhancement in the electrochemical properties of the functionalized graphene nanomaterials is in proportion to the amount of metal nanoparticles incorporated on the graphene nanosheets [86]. In this present work, silver and gold metallic nanostructure materials are used to modify the surface and interlayers of graphene nanosheets through physical deposition method.

1.7.2 Nobel metal nanoparticles

Metal nanoparticles are the substances that have been significantly employed for the modification of the sensor surface. The actual reason for employing metal nanoparticles for the surface modification is that, it acts as an electron mediator to generate the connection between the substrate and sensor surface [87]. Also it improves the following properties of the sensor materials:

- The mass transport properties
- The number of oxidation sites
- Heterogeneous electron transfer rate

- Sensitivity [88-89].

Various synthesis methods can be employed for the decoration of metal nanoparticles, which includes electro-deposition, electro-grafting, electro-polymerisation and drop-casting [90].

1.7.2.1. Silver nanoparticles

Silver nanoparticles are generally smaller than 100 nm in size and it is composed of 20 to 15000 silver atoms. Silver nanoparticles have some unique properties such as chemical stability, good conductivity, catalytic activity, optical property, thermal stability and antimicrobial activity. The thermal, optical and catalytic properties of silver nanoparticles strongly depend on their size and shape. They have wide range of applications in the medical field, textiles, food safety and personal care products [91].

Optical property

As silver nanoparticles are irradiated by specific wavelength of light, the scattering and absorption properties of these silver nanoparticles are changed in governing the shape, size and refractive index. Silver nanoparticles with smaller size mostly absorb light and produce UV-Vis absorption peaks near 400 nm. But the silver nanoparticles with larger size mostly produces scattering and UV-Vis peaks are shifted towards the larger wavelength [91].

Catalytic property

Among the numerous metal nanoparticles, silver nanoparticles (AgNPs) provide themselves as a useful substrate for the synthesis of chemically modified electrodes for electrochemical sensing due to its large specific surface area, high quantum characteristics of small granule diameter and the ability for fast electron transfer [92]. Due to this good catalytic nature, it has been used as a catalyst in medicinal applications. It also shows well defined redox property for benzene, dyes and carbon monoxide. It can also be used as a drug carrier for delivering various drugs and bio-molecules to specific targets [93].

1.7.2.2. Gold nanoparticles

Gold is one of rarest element on earth and its value has been known since days of yore. In addition to jewellery fabrication, gold has also discovered distinctive range of applications in various technologies. Gold is a Block D element in the group VI of Periodic table and it is a soft metal that is frequently alloyed to provide it with more strength. It has some unique nature: chemically inert, good conductor of electricity and heat and a good reflector of infrared radiation. Gold nanoparticles are also called as colloidal gold nanoparticles [94]. The morphological shape of gold nanoparticles is spherical, and they seem as a brown colour powder. The electronic and optical properties of gold nanoparticles can be modified by changing the shape, size, surface chemistry and aggregation state of gold nanoparticles. They have variety of applications such as sensory probes, organic photovoltaics, drug delivery in biological and medical applications, therapeutic agents, catalysis and electronic conductors.

Optical Properties

Colloidal gold nanoparticles have been employed for centuries by designers due to the vibrant colours generated by their interaction with the visible light. Depending on the particle shape, size, referactive index and aggregation state, it can absorb and scatter light radiation which results in change in colour which ranges from vibrant red to blue and black and finally to clear and colourless. These colour changes have been obtained due to the phenomenon of Localized Surface Plasmon Resonance (LSPR) [94]. The physico-chemical properties of gold nanoparticles are given in Table 1.2.

Table.1.2. Physico-chemical properties of gold nanoparticles

Properties	Values
Density	19.32 g/cm^3
Molar mass	196.97 g/mol
Melting point	1064.43˚C
Boiling point	2807˚C

1.7.3. Metallic compound nanostructures

Metallic compounds, specifically transition metal oxides (TMOs) or transition metal hydroxides (TMHs), are of essential materials in a variety of current demanding fields such as sensor, piezoelectric mechanics, optical electronics, energy storage and conversion, and catalysis, attributed to their unique functionality [95]. Because of these huge demands, metallic compound functionalized graphene nanosheets have been a current research topic in recent years. Generally, metal oxides and graphene nanosheets are produced separately and then functionalized through mixing of two (or more) components of metal oxide with graphene nanosheets via various physical and chemical methods. For example, pulsed laser deposition is employed to deposit metal oxide nanostructure materials on the graphene surface for specific functionalization to produce flexible energy storage devices and sensors etc., [96]. In some cases, functionalization of nanostructured metallic compounds with the graphene nanosheets is done only on the surface rather than the interlayers of the graphene sheets. In this present study, the metal oxide nanostructures are functionalized with graphene nanosheets through physical deposition method. Here, the metal oxide compounds such as zinc oxide and copper oxide nanoparticles are functionalized with the graphene nanosheets.

1.7.3.1. Zinc Oxide nanoparticles

In recent years, semiconductor nanoparticles have significant attention for their role in basic studies and technical applications [97] mainly due to their unique characteristics. Zinc oxide is a wide band-gap semiconductor material of the II-VI semiconductor group. It is an inorganic material with the chemical formula of ZnO. It is also known as zincite and usually obtains rarely in Earth crust. Due to the presence of manganese impurity, the element zinc actually appears as orange or red in colour. But the zinc oxide nanomaterials are usually appear as a white crystalline powder, which is insoluble in aqueous medium. Most of the commercial zinc oxide nanomaterials are manufactured synthetically and are widely employed as an additive into numerous products including ceramics, plastics, cement, rubber (e.g. car tyres), glass, paints, lubricants, ointments, sealants, adhesives, pigments, foods etc. Zinc oxide is a direct band gap semiconductor material with some unique properties such as good transparency, high electron mobility, high room-temperature luminescence, wide

bandgap for semi-conductivity, etc [97]. Due to these properties, zinc oxide has an emerging application in the field of energy-saving and heat-protecting windows, transparent electrodes in liquid crystal displays, thin-film transistors, ceramics plastics and light-emitting diodes.

Crystal structures

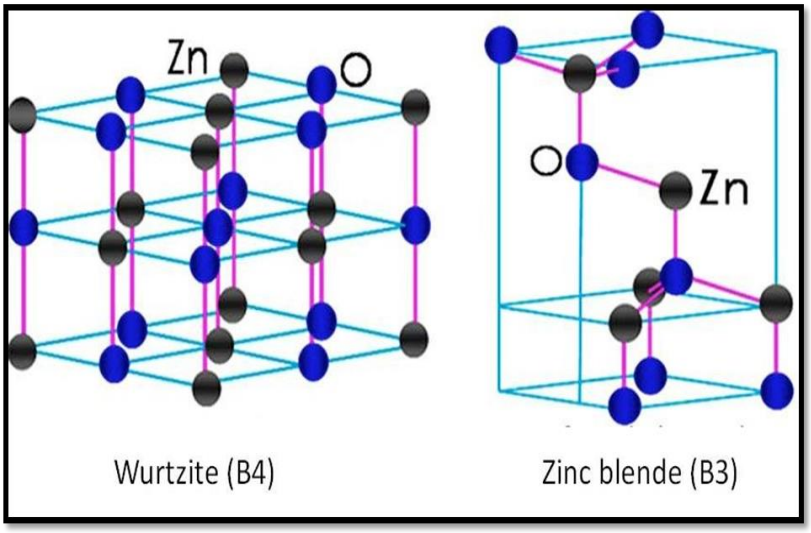

Figure.1.10. Structures of Zinc oxide

Zinc oxide usually crystallizes in two forms, (1) Hexagonal wurtzite structure and (2) Cubic zinc blende structure and is shown in the Figure.1.10. The wurtzite structure of zinc oxide is extremely stable under ambient conditions. The zinc blende structure can be stabilized by synthesizing zinc oxide on substrates with cubic lattice form. In both the forms of zinc oxide, the structure of zinc and oxide element is in tetrahedral shape [98]. The hexagonal and zinc blende structures of zinc oxide lattices have no inversion symmetry which results in the piezoelectricity and pyroelectricity of the hexagonal and zinc blende structure of zinc oxide. The values of the lattice constants are as follows:

- a = 3.25 Å;
- c = 5.2 Å;
- c/a ratio value is found to be 1.60 and is very close to the constant c/a value of hexagonal cell.

Physical properties

Zinc oxide has the following physic-chemical properties and is given in the Table1.3 [98-99]:

Table.1.3. Physicochemical properties of Zinc oxide

Properties	Nature
Colour	Multicrystalline solid: White Single crystalline solid: Colourless
Density	5.607
Molecular weight	81.37 C
Melting Point	1200˚C Under high pressure: 1975˚C Under low pressure: 1500˚C
Refractive Index	W=2.004, e=2.020
Band Gap	3.3 eV

1.7.3.2. Copper oxide nanoparticles

Over the past decades, the evolution of nanosized metal and metal oxide particles is significantly pursued due to their importance in various fields of applications. Generally, there is large number of metal oxides readily available in nature, but some of the metal oxide nanomaterials are most beneficial in accordance with their variety of applications in day to day life [94]. Among all the oxides of transition metals, copper oxide nanoparticles are of significant interest because of its high efficiency. The copper oxide nanoparticles are greatly employed for the applications of solar energy transfer, magnetic storage devices, sensors, chemical plants and super capacitors, etc. Copper (II) oxide or cupric oxide is the inorganic compound with the chemical formula of CuO [110]. It appears as a brownish black

powder, and it is also one of the two stable forms of oxides of copper. The other stable form of oxides of copper is being Cu_2O or cuprous oxide. As a mineral, it is called as tenorite. Copper oxide is obtained from copper mining and it is the fundamental precursor to many other copper-related products and chemical elements [94] [100]. It is widely employed in the field of superconductors, catalysis and ceramics, as a type of significant inorganic materials and it can also be employed as an electrode active materials as well as catalyst. The nanosized copper oxide has unique physical and chemical properties such as quantum size effect, surface effect and macroscopic quantum tunneling effect in optical absorption, magnetic, chemical activity, volume effect and thermal resistance that are superior than the regular copper oxide [101].

Structure

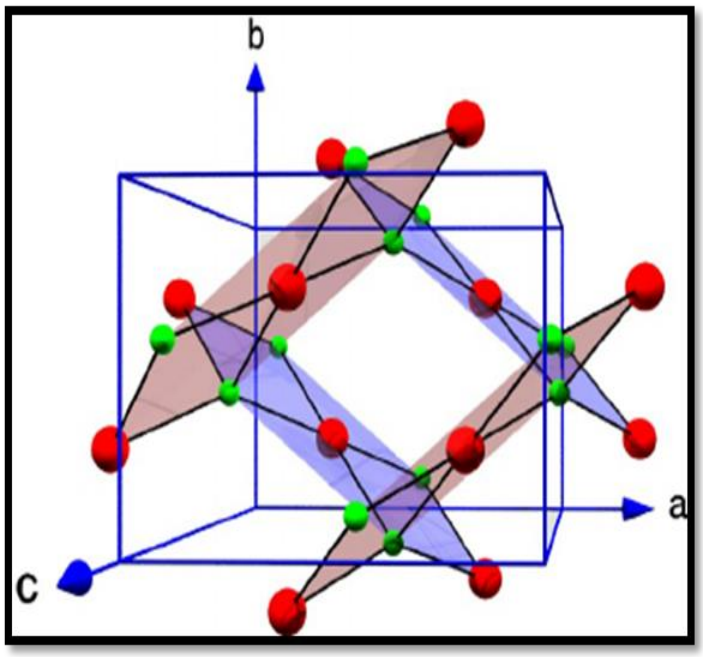

Figure.1.11. Structure of Copper (II) oxide

The structure of copper (II) oxide is monoclinic in which the copper atoms are coordinated by 4 oxygen atoms in a square planar configuration and is shown in the Figure.1.11 [94] [102].

Properties

- Thermal conductivity of water can be increased by the addition of copper oxide.

- ❖ It is a narrow band gap semiconducting material and employed for photo thermal and photoconductive applications.
- ❖ It has a metallic property in bulk form and it acts like a semiconductor material in nano scale level.
- ❖ It behaves as a catalyst, whereas all the other metal oxides are not beneficial for the catalytic activity.
- ❖ It can also be used for the fabrication of super capacitors [94].
- ❖ It has the large band gap value relatively equal to zinc oxide. The wide band gap value of copper oxide is found to be around 2.6 eV, makes it beneficial for solar energy conversion.
- ❖ Melting point and density of copper oxide nanoparticles is 1326 $^{\circ}$C and 6.3-6.49 g/cm^3, respectively.
- ❖ It is soluble in diluted acids, potassium cyanide solution and NH_4Cl and it is insoluble in aqueous medium and also it slowly dissolves in alcohols and ammonia solution [101].

1.8. POLYMERS

Besides metal and metal oxide nanocomposites, polymer-functionalized graphene nanosheets also have widely been employed for sensor, storage and energy conversion applications. In this present work, a highly conductive Beta-cyclodextrin polymer (β-CD) is used for functionalization with graphene based nanomaterials. The as-prepared polymer functionalized graphene based nanocomposites are electrochemically active and enabled to accommodate metallic and metallic compound nanostructure materials.

1.8.1. Cyclodextrin polymer

Cyclodextrin is familiar over 100 years and it has a major effect in the field of pharmaceutical [103-105]. It is first described by a French scientist Villiers. In his description, cyclodextrin is known as a crystalline substance detached from the bacteria Bacillus macerans by digestion of starch [106-107]. They are non-reducing, water

soluble macrocyclic oligosaccharides consisting of six to twelve glucopyranose units connected by α 1, 4- linkages. Cyclodextrins with six, seven and eight glucopyranose monomers are assigned as α, β and γ cyclodextrin respectively [108] and are shown in the Figure.1.12.

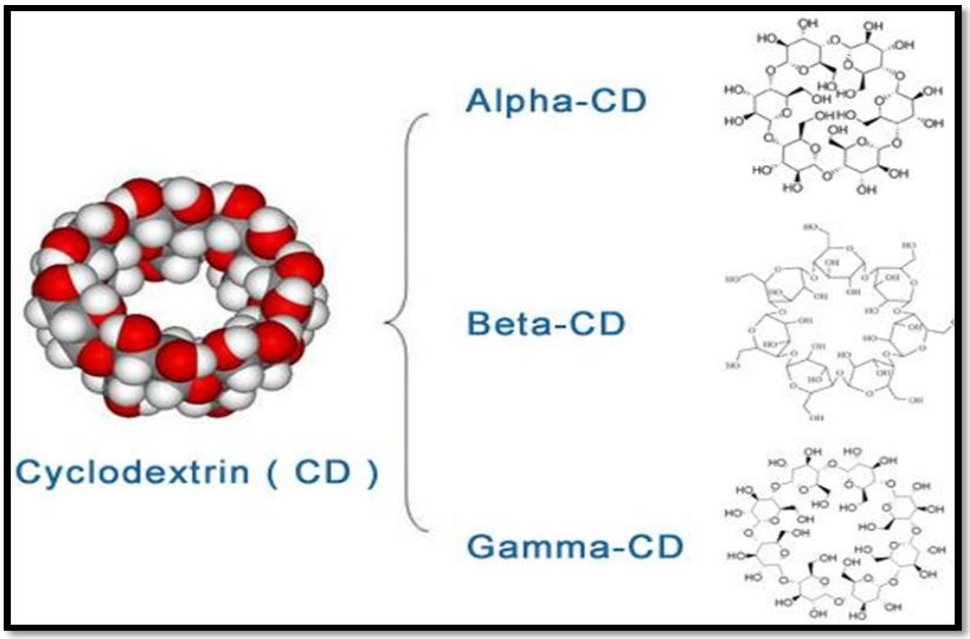

Figure.1.12. Types of cyclodextrin polymer

They are also named as cycloamyloses, cyclomaltoses and Schardinger dextrins. They are toroidal in shape featuring great potential to entrap completely or at least partially a large scale of branched as well as unbranched drug molecules. The hydrophobic inner surface and hydrophilic external surface makes cyclodextrin as essential organic compounds. Cyclodextrins are more efficient to form stable and soluble non covalent bonds with host-guest molecules.

The ring structured molecules of cyclodextrin confines a cavity size of about 6, 8 and 10 A˚ in diameter for α, β and γ cyclodextrin respectively [109-110]. The interior cavity of the cyclodextrin molecules is generally hydrophobic in nature because of the presence of CH_2 functional groups, and the nature of the exterior cavity is hydrophilic, due to the presence of primary and secondary hydroxyl functional groups. The molecules with the appropriate size, shape and stereochemistry could be able to intercalate with the exterior cavity of cyclodextrin molecules by the Vander waalls force

of attractions and by the hydrophilic nature. The ability to produce inclusion complexes in aqueous medium is due to the typical alignment of the glucose units [111-112].

Electrocatalytic properties

One of the most distinct properties of conducting polymers is their potential to catalyze electrode reactions. Thin layers of a conducting polymer deposited onto the surfaces of electrodes are able to enhance the kinetics of electrode processes of some solution species. This kind of enhancement in the electrocatalytic processes of conducting polymer electrodes shows an impact on the unexpected applications in various fields of applied electrochemistry.

In conducting polymer modified electrodes, three processes are considered to take place during electrocatalytic conversion of solution species. The first process is the heterogeneous electron transfer between the electrode and the conducting polymer layer, and electron transfer within the polymer film. This process is accompanied by the movement of charge compensating anions and solvent molecules within the conducting polymer film, and possible confirmational changes of polymer structure as well. The rate of this process is determined by many factors. Among these, electrical conductivity of the polymer layer, electron self exchange rates between the chains and/or clusters of polymer, and anion movement within the polymer film are of great importance. The second process is the diffusion of solution species to the reaction zone, where the electrocatalytic conversion occurs. As compared to simple electrode reactions, this process can be more complicated in cases where the electrocatalytic conversion occurs within the polymer film due to the fact that the diffusion of species within the film, as well as the possible electrostatic interaction of this species with the polymer itself should be taken into account. The last process is represented by the actual chemical (heterogeneous) reaction taking place between the solution species and the conducting polymer.

From both the theoretical and practical points of view, the question on the field of electrocatalytic process seems to be of primary interest. If the charge transfer within the layer of conducting polymer proceeds much faster than the mass transfer of reacting species and their electrochemical conversion then the electrocatalytic process should proceed at the outer conducting polymer/solution interface. In an opposite case, if the

mass transfer and electrochemical reaction proceed faster than the electron transfer in the conducting polymer, an electrocatalytic process occurs at the inner substrate electrode/conducting polymer interface, assuming that the permeability of a porous conducting polymer layer is sufficiently high to penetrate the reacting species and solution ions. Finally, if both processes occur at comparable rates, the electrocatalytic process is located within the conducting polymer layer. The depth of the reaction zone within the conducting polymer layer can be determined by the balance between charge and mass transfer, and the rate of electrocatalytic conversion as well. Based on the described processes, the electrocatalysis at conducting polymer modified electrodes can be subdivided into two main categories:

- Metal-like electrocatalysis occurs at conducting polymer/solution interface at a high conductivity of electrode material. In this case, an overall rate is determined by the flux of solution species, or by the rate of catalytic conversion.

- Redox catalysis occurs within the polymer layer, or at inner substrate electrode/conducting polymer interface at a limited conductivity of the modifier layer [113-114].

1.9. FUNCTIONALIZATION OF POLYMER

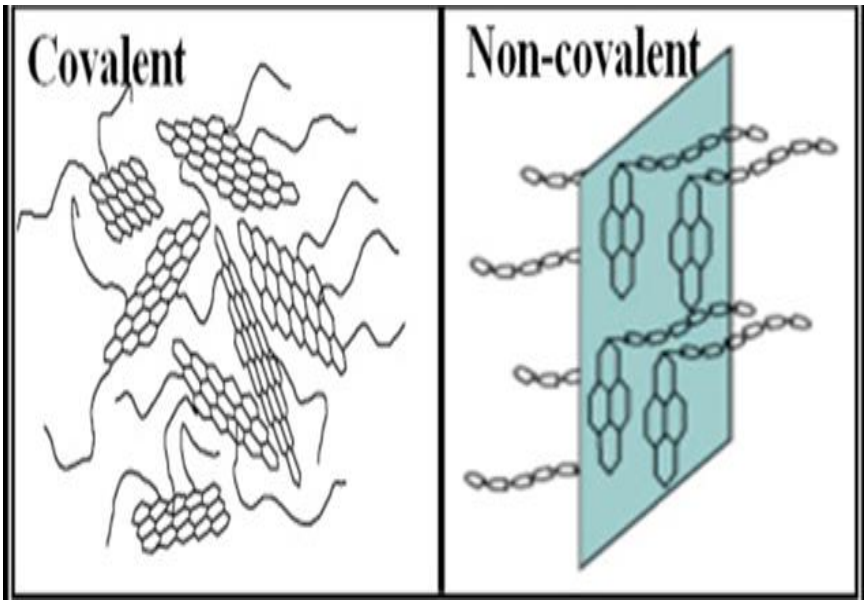

Figure.1.13. Types of functionalization of polymer

The Figure.1.13 represnts the covalent and non-covalent functionalization of polymer matricies with graphene nanosheets and are described as folows:

1.9.1. Covalent bonding

Graphene nanosheets consists of notable number of oxygen-containing functional groups, which provides significant opportunities for further modification with polymer either by 'grafting to' or by 'grafting from' methods through covalent bonding. Covalent functionalization of polymer matrices with the graphene nanosheets is mainly figured out through the interaction between the oxygen-containing functional groups of graphene nanosheets and the active functional groups of the polymer matrices such as $-NH_2$ and –OH [115].

1.9.2. Non-covalent bonding

Non-covalent functionalization of polymer matrices with graphene nanosheets are done through the π-π stacking interaction or by the electrostatic interaction of active functional groups of polymers with oxygenated functional groups of graphene nanosheets. Large scale of polymer matrices such as poly (sodium 4-styrenesulfonate), polyaniline and poly (p-phenylene vinylene) are included into graphene nanosheets with a unique functionality and homogenous multilayer structure. The graphene nanosheets show high performance of responses to moisture, heat and light by functionalizing it with polymer materials [116-117].

1.10. APPLICATIONS

The various electrochemical sensor applications of graphene based nanomaterials are shown in the Figure.1.14. Graphene based nanomaterials have been employed in electronic and opto-electronic devices, sensors, electrochemical energy devices and water treatment due to its unique nature such as low price, high quality and simple synthesis process.

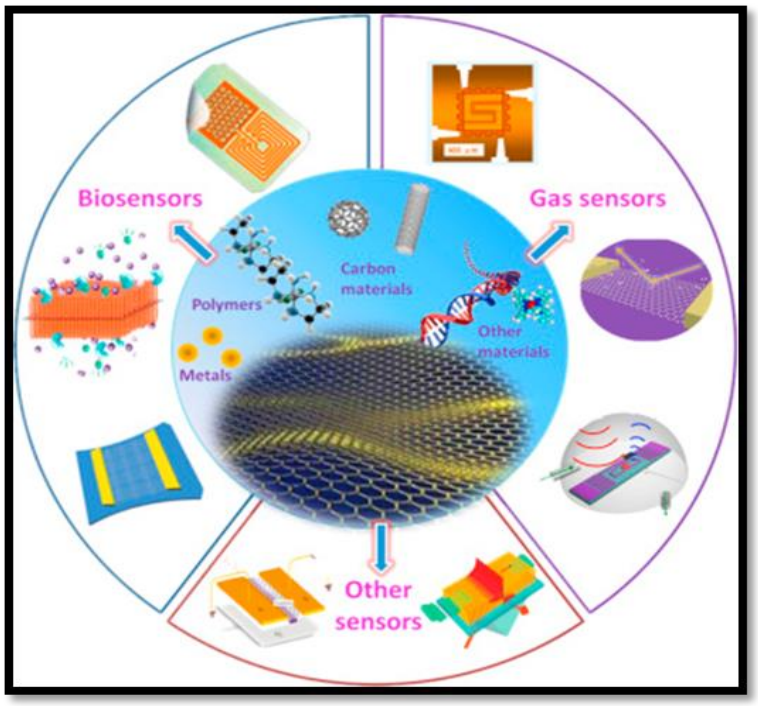

Figure.1.14. Application of graphene based nanomaterials

Typically, the self-assembled 2-D graphene nanosheets functionalized with nanostructured metals, metal oxides, polymers and biomolecules are promising electrode materials for sensing applications. Electrochemical sensors with high sensitivity have found widespread uses in clinical diagnosis, environmental monitoring and for quality control in food, agricultural products. [95] [118-122].

1.10.1. Graphene-Enzyme based sensors

Graphene sheet based nanomaterials showed tremendous physical and electrochemical properties, such as large surface area, high conductivity, superior electrocatalytic activity, abundant defect sites and fast electron transfer rate. Hence, different enzyme based electrochemical sensors are fabricated based on this excellent material. It shows reasonable stability and good anti-interference ability [123-124].

1.10.2. Non-enzymatic sensors

In most kind of amperometric electrochemical sensors, enzyme modified electrode material is employed for the electrochemical detection of analytes. The enzyme modified graphene nanomaterials activates the catalytic oxidation of analytes with high sensitivity and selectivity. Although, enzyme-modified electrodes have some

drawbacks such as less reproducibility, high anti-interference ability, high cost of enzymes and complicated enzyme immobilization. To overcome such issues, non-enzymatic electrochemical sensors based on graphene nanosheets are explored. Hence, metal oxide nanostructured material based graphene nanosheets showed a high performance for the production of electrochemical sensors due to the presence of oxygenated compounds in the metal oxides nanostructures. These oxygenated functional groups are able to perform electrochemical reaction with the analytes, resulting in an incredible enhancement in the electrochemical properties. Several experiment studies have confirmed that the metal oxide nanomaterials functionalized graphene nanosheets can effectively detect analytes without any biological elements. For example, copper oxide, a p-type semiconductor with a narrow band gap value of 1.2 eV, is an extremely promising material for the fabrication of glucose sensors [125]. This kind of sensing platform displayed a reasonable stability and good anti-interference ability due to the good electrochemical activity, high specific surface area and the probability of stimulating electron transfer reactions at a lower potential range.

1.10.3. Electrochemiluminescence sensors

Electro-chemiluminescence (ECL) is a type of luminescence caused by the electrochemical reactions at liquid / solid interfaces. Electro-chemiluminescence method is found to be one of the highly sensitive and selective techniques in analytical science. This method integrates the advantages of chemi-luminescent techniques by applying an optimized electrode potential. Hence, Electro-chemiluminescence based sensors are freshly developed using graphene based nanomaterials. For example, l de-hydrogenase-modified graphene nanosheets / bovine serum albumin nanocomposite film is developed for the detection of ethanol. Electro-chemiluminescence sensor also displayed a high selectivity, long-term stability and good reproducibility [126].

1.10.4. Immunosensors

Immunosensors are one of the most significant sensors for biomedical applications. Due to high conductivity and flexibility, the fabrication of graphene nanosheets based electrochemical immunosensors is highly useful [127]. For example, a facile and label-free electrochemical impedimetric immunosensor are developed for the detection of immunoglobulin G (IgG) based on chemically modified graphene

nanosheets. In another case, facile and low cost impedimetric immunosensor is developed for the rapid detection of Escherichia coli O157:H7 (E. coli O157:H7) by using gold nanoparticles-functionalized graphene sheet electrodes.

1.11. CHARACTERIZATION TECHNIQUES

Various instrumental techniques are available for the characterization of synthesized graphene oxide nanosheets, beta-cyclodextrin functionalized reduced graphene oxide nanosheests, metal (silver, gold) nanoparticles decorated beta-cyclodextrin functionalized reduced graphene oxide nanosheets and metal oxide (CuO, ZnO) nanoparticles decorated beta-cyclodextrin functionalized reduced graphene oxide nanosheets to examine the functional, structural, morphological and sensing property of nanocomposites. The techniques employed to characterize these nanocomposites are:

- **Fourier Transform Infrared spectroscopy (FT-IR)**
- **X-ray Diffraction analysis (XRD)**
- **Scanning Electron Microscopy (SEM)**
- **Energy Dispersive X-ray spectroscopy (EDAX)**
- **High Resolution Transmission Electron Microscopy (HRTEM)**
- **Cyclic voltammetry (CV)**

1.11.1. FT-IR spectroscopy

Fourier Transform-Infrared spectroscopy is a characterization technique employed to determine the vibration features of the chemical functional groups in the samples by attaining an infrared spectra of absorption, emission of the samples [128]. In this research work, infrared spectra are recorded using a Shimadzu FT-IR spectrometer. The scanning wavelength of this FT-IR spectrometer ranges from far infrared region (400 cm^{-1}) to mid infrared region (4000 cm^{-1}) and it employs a single reflection horizontal extenuated total reflection component that enables the sample to be investigated directly in the solid or liquid form without additional sample preparation [129]. The working principle of this type of spectrometer is described as follows:

When an infrared radiation irradiates the sample surface, it induces the changes in the vibrational energy modes of molecule in the form of stretching, bending and contracting motions. The absorption of IR energy induces the oscillation in the dipole moment of the chemical compound that corresponds to the specific vibrational modes and it is also directly proportional to the square of the dipole moment of the chemical compound. These vibrational modes are related to the specific energies and are distinct for every functional group of the chemical compound. The recorded FT-IR spectrum may be employed as a distinctive fingerprint of a chemical compound. The vibrational modes between two distinctive atoms can be estimated by Hooke's law [130]. In this estimation, two atoms and the linking bond are considered as a simple harmonic oscillator, where the frequency corresponds to two quantities such as a force constant and the masses of the atoms are as given by the Equation

$$v = 12\pi\sqrt{km} \qquad \text{..... (1)}$$

Where v is the frequency of the vibration between the two atoms, k is the force constant and m is the mass of the chemical compound. This describes that the bigger atoms vibrate slower than the smaller atoms and also how bonds with a greater degree of saturation vibrate at larger wavenumbers.

1.11.2 X-ray diffraction analysis

X-rays are known as electromagnetic radiation of wavelength ranges between 0.1 Å to 100 Å, which lies in the region of Gamma rays and Ultraviolet rays, and are in the domain of short interatomic bonds [131]. X-ray diffraction method is employed for characterizing the degree of crystallinity in solid samples, as well as diagnosing the individual phases that exists. In this present work, X-ray Diffraction (XRD) is employed to determine the change in the inter-layer spacing between the graphene nanosheets and to find the crystalline nature of the metal and metal oxide nanoparticles, that is used to decorate the surface and inter-layers of graphene oxide nanosheets. All the X-ray diffraction patterns given in this present research are carried out using a Shimadzu XRD 6000 Advance powder X-ray diffractometer equipped with a Vantec-1 detector operating at 40 kV and 30 mA. It operates on the phenomena that, when X-rays are passed through the samples, it interferes with the array of atoms in a constructive,

destructive or partially destructive aspect. And the interaction of X-rays with the samples strongly depends on the arrangement of atoms and their relative distance [132].

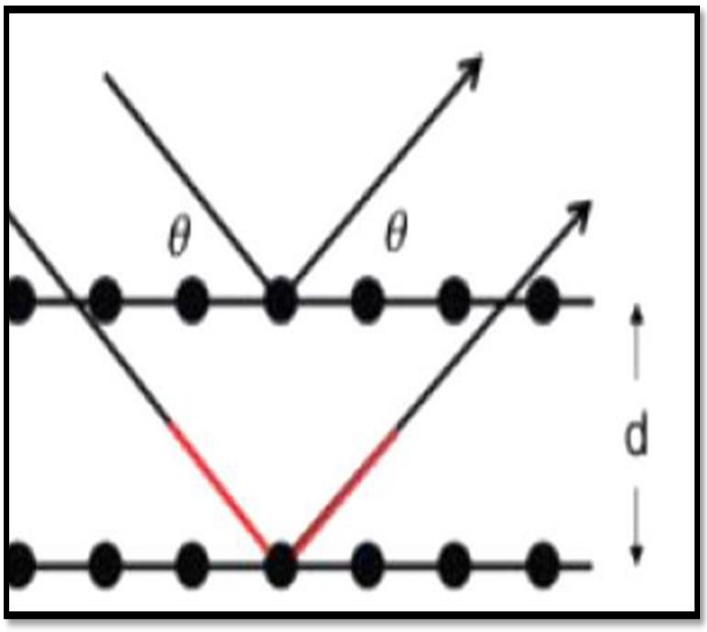

Figure.1.15. X-ray diffraction on a two-plane system

The X-ray which interferes with the atoms of the samples may get diffracted in a different angle and these diffracted angles eventually give the information about the array of atom using the Bragg's law of equation. Figure.1.15. shows the simple demonstration of Bragg's law enforced on two planes with periodically placed atoms. Bragg's law is an important phenomena used to describe the conditions essential for the constructive interference.

$$n\lambda = 2d\sin(\theta) \qquad \text{.....(2)}$$

Where n is the order of diffraction, λ is the wavelength of the X-rays, d is the inter-atomic distance and θ the incident angle of the X-ray on the samples [132] [133].

1.11.3. Scanning Electron Microscopy

Scanning electron microscopy (SEM) is an eminent technique employed for the investigation on the morphology of microstructure of the samples. Jeol JSM 6390 model scanning electron microscope is employed for the morphological analysis of all the samples in this present research work. This type of scanning electron microscope

employs electrons rather than light to produce an image. In comparison to conventional microscopes, scanning electron microscope has abundant advantages such as higher resolution, large depth of field and effective control over the degree of magnification [134], which permits it to be employed in microstructure investigation, fracture characterization, surface contamination investigation, thin film examination and failure detection of the materials. The samples to be investigated are deposited in the vacuum chamber of the electron microscope. The scanning electron microscope is driven with an operating energy of 30 keV, size of the electron beam at a value of 3 and an operating distance of about 10 mm. The morphological images of the samples at different magnifications are captured. This kind of scanning electron microscope produces the high resolution micrographs of nanoparticles surface to discover the information about topography and morphology and it operates based on the following principle. The high resolution micrographs are generated by using a high-energy electron beam which is produced from the electron gun in an evacuated chanmber and it is allowed to bombard with the sample surface [135]. When the electron beam falls onto the sample surface, the low-angle backscattered electrons are able to interact with the atoms on the surface of the sample and produce a variety of electronic signals. These electronic signals are then collected using a positive detector which analyses, amplifies and translates the electron signal into micrographs. The accelerating voltage used to generate electron beams are ranging from 1 to 30 kV. This kind of scanning electron microscope uses magnetic lenses and scan coils to focus and scan the electron beam on the sample material. The pressure generated on the sample chamber is varied from 10^{-3} - 10^{-5} Pa [136].

1.11.4. Energy Dispersive X-ray analysis

Energy dispersive X-ray characterization (EDAX) analysis approves the confined micro-elemental study of the top few micrometres of the sample surface. X-ray radiations are produced, when the high-energy electron beam hits the inner shell electron of the sample surface. Every element in the sample has its own typical orbital energies and the X-rays emitted by the element in the sample are connected to its chemical composition. EDAX spectra contain a series of elemental peaks located at distinct energies depending on the chemical element. The intensity of the elemental peak is found to be proportional to the number of elements present in the specimen and

the energy of the emitted X-ray. The emitted X-rays are then focused onto the EDAX detectors [137]. There are two types of detectors available such as silicon drifted detector (SDD) and lithium-drift silicon detectors. A quantitative EDAX characterization is applicable only with quality rich flat-polished sample surfaces. The quantitative investigation is feasible by the comparison of respective peak heights of the standard of known composition measured and the sample under the similar conditions [138].

1.11.5. High Resolution Transmission Electron Microscopy

High resolution transmission electron microscope is an instrument technique employed for the high-magnification investigations on nanomaterials. High resolution makes it ideal for imaging samples on the atomic scale level. A major benefit of a transmission electron microscope over other types of microscopes is that it can concurrently provide information in real space as well as in reciprocal space. In this study, JEOL JEM 2100 model is employed to generate higher resolution transmission electron microscope (HRTEM) images. This kind of transmission electron microscope employs a beam of electrons to produce a high resolution images by transmitting the electron beams through the surface of ultra thin specimen. The as produced micrograph is then magnified and focused onto imaging equipment, such as on a layer of photographic film, or on a fluorescent screen. Then the collected electron beams are detected by using a sensor device such as a charge-coupled device (CCD) camera [139]. It has an isolated tilt stage and has a maximum tilt angle of -10˚ to +10˚ in Goniometer. The transmission electron microscope can work in bright, dark, high resolution, SAED and CBED modes. This type of TEM instrument has a standard and a variable temperature probe (100 to 500 K). For digital image processing, this TEM instrument is coupled with a Gatan digital camera. This type of instrument can go upto a highest magnification value of 1.5 million. It has an anti contamination device employed with the help of liquid nitrogen, which assists the filament from contamination. A fundamental phenomenon of TEM is relatively similar to the operating principle of optical microscope. The main difference is that in transmission electron microscope, a focused electron beams are used instead of light to produce an image and gives the information about the morphological structure and composition of the sample.

1.11.6. Electrochemical analysis

An electrochemical experiment such as cyclic voltammetry (CV) is investigated using instrument named as Biologic SPF 150 interfaced to a Lenovo computer system. In this research work, all experimental investigations are carried out using a typical three-electrode system.

Electrochemical cell

The schematic representation of electrochemical cell is shown in the Figure.1.16 and it is a standard three-electrode cell contains a working electrode (WE), an auxiliary or counter electrode (CE) and a reference electrode (RE). The bare and synthesized nanocomposites modified glassy carbon electrode acts as a working electrode, a platinum wire as an auxiliary electrode and an Ag/AgCl rod as a reference electrode.

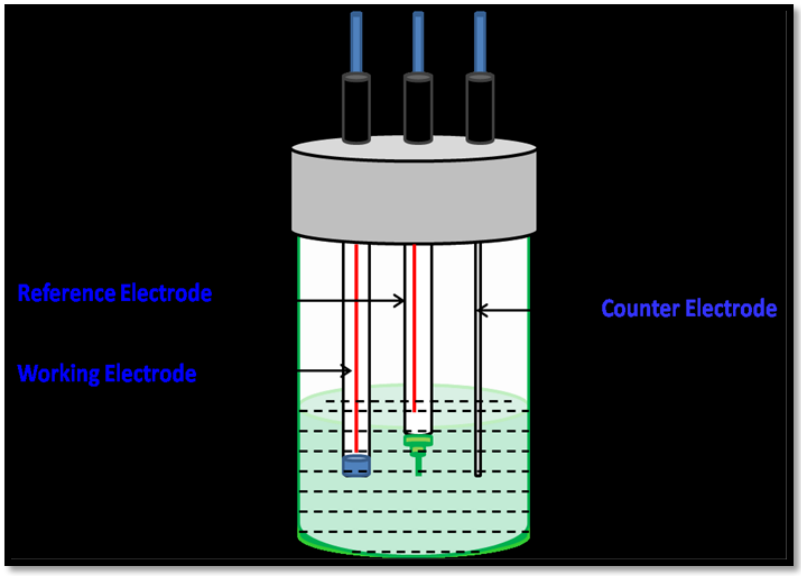

Figure.1.16. Electrochemical cell setup

All three electrodes are coupled with the potentiostat using shielded wires. The potential applied to the working electrode is governed with respect to the reference electrode and the reference electrode is located as close to the modified working electrode as possible to decrease the ohmic potential dip. The current flows between the auxiliary and working electrode. All the obtained potentials are recorded vs. Ag/AgCl reference electrode at room temperature and stored on a standard computer [140].

Reference and auxiliary electrodes

The Ag/AgCl is used as reference electrode and it contains a silver wire glazed with silver chloride material. The silver chloride coated silver wire is then immersed in a 3 M of potassium chloride solution (KCl) as shown in the Figure.1.16. As there is a huge chloride concentration slope over the reference electrode region, the diffusion of chloride ions from the reference electrode into the same solution is slow. Hence, the reference electrode must be immersed in a 3.0 M of potassium chloride solution between the experiments. The air bubbles generated in the KCl solution, next to the frit can be eliminated by softly taping the end of the electrode or else excessive noise may produce in the analytical data while performing voltammetric experiments [141].

1.11.7. Cyclic voltammetry

Cyclic voltammetry (CV) is generally the primary technique employed to characterize an electrochemical reaction which provides essential information on the reaction mechanism. Cyclic voltammetry concerns the cycling of the applied potential at the working electrode and monitoring the resulting current. The initial potential (E_i) is cycled to a vertex potential (E_v) and then the scan reversed and cycled back to the final potential E_f, which is generally same as the applied potential (E_i). These sweeps are basically repeated for large number of times and at a constant rate named as the scan rate. The resulting data is plotted as applied potential (V vs. ref) vs current measured (A cm^{-2}). The working electrode acts as the surface whereas the redox reaction takes place and the electrical current generated is described as the faradaic current. There are four major cyclic voltammetry responses that strongly correspond to the reversibility of the redox mechanism and are shown in the Figure.1.17, 1.18, 1.19 and 1.20.

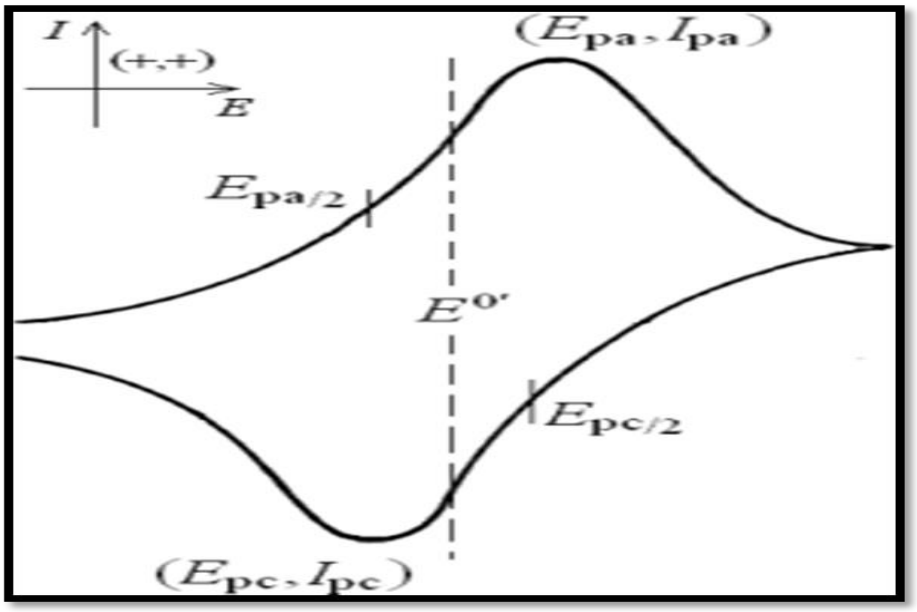

Figure.1.17. Reversible redox reaction

Ep independent of υ

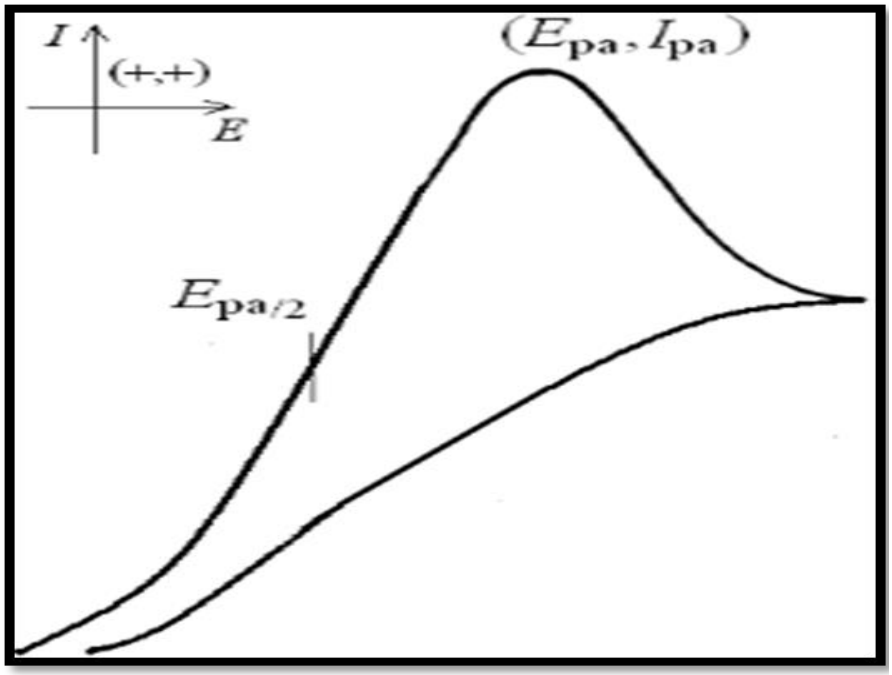

Figure.1.18.Irrevesible redox reaction

$|Ep|$ increases as υ increases

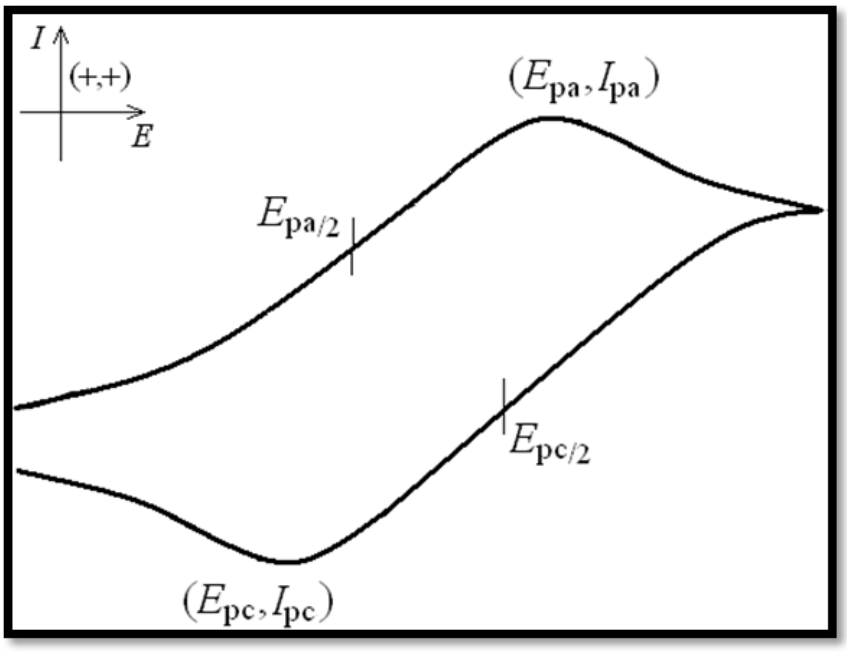

Figure.1.19. Quasi reversible redox reaction

I_p not prooportional to square root of scan rate

E_p increases as scan rate increases

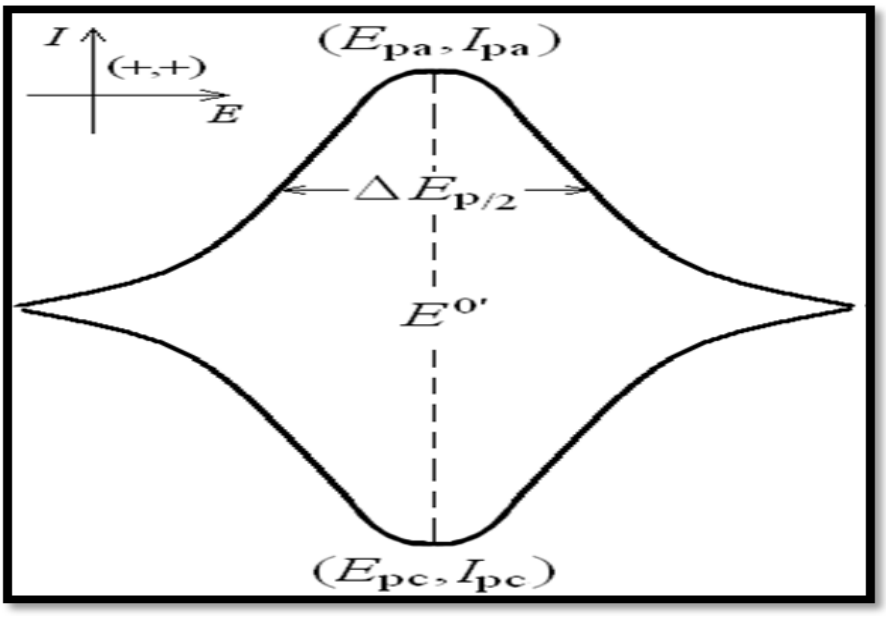

Figure.1.20.Adsorption redox reaction

$I_p \alpha \upsilon$

E_p independent of υ

Every redox response is analyzed by the various shape of the respective cyclic voltagramm, which is defined by the following three parameters, the peak potential (E_p), the peak current (I_p), and the half peak potential width ($E_p - E_{p/2}$). The peak potential E_p does not affected by the scan rate for the reversible systems. The changes in the peak current I_p is linearly proportional to the square root of the scan rate for the reversible and irreversible systems. The cyclic voltagramm response at various scan rates discovers the kinetic information concerning the electrocatalytic process such as diffusion and adsorption effects [142].

1.12. OBJECTIVE OF THE PRESENT WORK

An extensive literature survey is performed on the graphene and its surface modifying nanocomposites such as polymer membranes and metal/metal oxide nanoparticles for its various applications. Graphene and its derivatives have received much attention because of its unique properties such as high conductivity, high surface area and low cost of production and the modifications of graphene surface with polymer membranes and metal/metal oxide nanoparticles will enhance the properties of graphene derivatives. Hence, in the present study, Beta-cyclodextrin (β-CD) polymer has been chosen as it have very peculiar properties such as drug inclusion capability, stability, host-guest recognition ability, hydrophobicity and also metal/metal oxide nanoparticles that have high conductivity and high specific surface area, as a graphene surface modifiying material. These properties made graphene and its surface modifidied nanocomposites as a most suitable nanomaterial for the electrochemical sensor applications.

Nitrophenols (NPs) are commonly used in the manufacturing of pesticides, dyes, pharmaceuticals and explosives. The nitrophenol isomers such as ortho-nitrophenol (o-NP), para-nitrophenol (p-NP) and meta-nitrophenol (m-NP) have momentous toxic effects on human beings, mammals, microorganisms and plants. Hence, the detection of nitrophenols is of extreme importance, since it is noticed as pollution abatement. There are diverge instrumental techniques that are frequently employed for the determination of nitrophenols. In this present work, the electrochemical method based on chemically modified electrode is employed for various analytical determinations, due to their cost effectiveness, sensitivity, high efficiency and simplicity.

Hence, the objective of the present work is to synthesize metals (Ag, Au) / metal oxides (ZnO, CuO) nanoparticles embellished β-cyclodextrin functionalized reduced graphene oxide nanocomposites of various concentrations and to investigate the electrochemical sensing properties towards the detection of nitrophenol isomers such as ortho-nitrophenol (o-NP), para-nitrophenol (p-NP) and meta-nitrophenol (m-NP).

To accomplish the objective of the present work, the following steps are employed:

- Synthesis of graphene oxide nanosheets via modified Hummer's method.
- Chemical functionalization of reduced graphene oxide nanosheets using β-cyclodextrin polymer through chemical reduction method.
- Surface modification of polymer functionalized reduced graphene oxide nanosheets using various metal (Ag, Au) and metal oxide (ZnO, CuO) nanoparticles via wet chemical method.
- Investigation on the physical properties of synthesized graphene based nanocomposite through FT-IR, XRD, SEM, EDAX and HRTEM with SAED analytical techniques.
- Electrochemical investigation on the detection of nitrophenol isomers using various metal (Ag, Au) and metal oxide (ZnO, CuO) nanoparticles embellished β-cyclodextrin functionalized reduced graphene oxide nanosheets.
- Evaluation on the electrocatalytic activity of unmodified graphene oxide nanosheets, β-cyclodextrin polymer functionalized reduced grpahene oxide nanosheets and various metal (Ag, Au) and metal oxide (ZnO, CuO) nanoparticles embelished β-cyclodextrin polymer functionalized reduced grpahene oxide nanosheets towards the detection of nitrophenol isomers.

Based on the objectives, this present research work is carried out and the results are discussed in their respective chapters.

1.13. ORGANIZATION OF THESIS

This thesis consists of 8 chapters, each having its own introduction and reference.

CHAPTER I describes about the nanoscience and technology and its tremendous use in the field of sensors, biomedical, electronic and solar applications, etc. It explains the basic physio-chemical properties of materials used in this work such as graphene and its allotropes, polymer matrix, metals (silver, gold) and metal oxides (zinc oxide, copper oxide) nanocomposites. This chapter elucidates the influence of β-cyclodextrin polymer used for the surface modification of graphene oxide. It also describes the importance of metals and metal oxides used to enhance the surface property of β–CD functionalized graphene oxide. It outlines the literature survey studied to design the nanomaterials used for the applications and also clearly illustrates the instruments used for the characterization of synthesized nanomaterials. Furthermore, this emphasizes the electrochemical system which opens up the way of nanotechnology in sensor fields.

CHAPTER II outlines the synthesis methodology of graphene oxide nanosheets by Modified Hummer's method and the chemical functionalization of graphene oxide nanosheets with the β-cyclodextrin polymer via chemical reduction method. It also describes the synthesis of various metal (Ag, Au)/ metal oxides (ZnO, CuO) nanoparticles embellished β-cyclodextrin functionalized reduced graphene oxide nanosheets through wet chemical method.

Chapter III explains the synthesis of graphene oxide nanomaterial through modified Hummer's method using natural graphite powder. The functional, structural, morphological, elemental composition and electrochemical sensing properties of synthesized graphene oxide are studied using Fourier Transform Infrared spectroscopy (FT-IR), X-Ray diffraction (XRD), Scanning electron microscopy (SEM), energy dispersive X-ray (EDAX), High resolution transmission electron microscopy (HR-TEM) and Cyclic voltammetry techniques (CV). This chapter describes the layered structured morphology of synthesized graphene oxide nanomaterials. It also clearly illustrates the electrochemical sensing behaviour of graphene oxide examined for the different nitrophenols in phosphate buffer solution by cyclic voltammetry analysis.

Chapter IV elucidates the synthesis of different concentrations of silver nanoparticles decorated β-cyclodextrin functionalized graphene oxide nanocomposites. The formation of well crystalline nature of silver nanoparticles on the surface of GO-β-CD nanosheets by XRD analysis is described. The decoration of silver nanoparticles on the GO-β-CD surface for the various concentrations of silver nanoparticles are discussed from SEM analysis and that distribution of silver nanoparticles play a crucial role in the investigation of electrochemical sensing of nitrophenols.This chapter also describes the cyclic voltammetry studies examined for the detection of nitrophenol such as o-NP, p-NP and m-NP at different pH of phosphate buffer solution. The synthesized nanocomposites showed the best electrochemical behaviour for the detection of ortho-nitrophenol compound.

Chapter V outlines the influence of different concentration of gold nanoparticles on the surface of GO/β-CD nanosheets. It discusses the functional, structural, morphological properties of synthesized nanocomposites by the investigation of FT-IR, XRD, SEM and HRTEM techniques. This describes the sphere shape morphology of gold nanoparticles that are deposited on the surface of GO/β-CD nanosheets. The morphological analysis also shows that the gold nanoparticles are decorated uniformly without any agglomeration for the lower concentrations such as 0.002 M to 0.006 M. For the higher concentrations such as 0.008 M and 0.01 M, the gold nanoparticles are found to be agglomerated on the GO/β-CD surface. This morphological investigation plays the crucial role in the electrochemical detection studies. The electrochemical investigations for three different nitophenols (o-NP, p-NP and m-NP) are carried out for all the concentration of GO/β-CD/Au nanocomposites. It shows the good electrochemical sensing behaviour for the lower concentration of gold nanoparticles that are deposited without agglomeration. The synthesized nanocomposites showed the best electrochemical behaviour for the detection of ortho-nitrophenol compound.

Chapter VI focuses on the various concentrations of zinc oxide nanoparticles intermediated on the surface of β-cyclodextrin functionalized graphene oxide nanocomposites. This chapter figures out the investigations carried out to examine the properties such as functional, structural, morphological, and elemental composition of synthesized nanocomposites by FT-IR, XRD, SEM, EDAX and HRTEM with SAED

techniques. The obtained high crystalline miller indices of the synthesized nanocomposites are well matched with the JCPDS card no (36-1451). The crystallite size of the zinc oxide nanoparticles is found to be linear for the concentrations from (0.002 M-0.008 M) of zinc. The crystallite size affects the sensing property of GO/β-CD/ZnO nanocomposites. The electrochemical studies carried out for the three different nitrophenol compounds (o-NP, p-NP and m-NP) shows the better sensing behaviour for the zinc oxide nanoparticles with smaller crystallite size. The synthesized nanocomposites showed the best electrochemical behaviour for the detection of para-nitrophenol compound.

Chapter VII emphasizes the disparate concentrations of copper oxide nanoparticles mediated β-cyclodextrin functionalized graphene oxide nanocomposites. The morphological properties of the samples show the spherical shape of copper oxide nanoparticles on the surface of functionalized graphene oxide. The cyclic voltammetry study reveals the detection property of copper oxide nanoparticles for the three different nitrophenols (o-NP, p-NP and m-NP). The synthesized copper nanoparticles showed better nitrophenol sensitivity for the 0.004 M concentration of copper, due to the maximum number of copper nanoparticles with feeble agglomeration on the surface of functionalized graphene oxide. The synthesized nanocomposites showed the best electrochemical behaviour for the detection of para-nitrophenol compound.

Chapter VIII concludes with the summary of the results and scope for the future research work.

References

1. C. P. Poole, F. Owens, Introduction to nanotechnology, Springer Hand book of Nanotechnology, (2003).
2. A matter of Size: Triennial review of the national nanotechnology initiative, National Academy Press, Washington DC, (2002).
3. Nanoscience and nanotechnologies: opportunities and uncertainties, Nanoscience and nanotechnologies report by The Royal Society and The Royal Academy of Engineering, (2004).
4. C. Ralph, C. Merkle, Computational nanotechnology, J. Nanotechnology, 2, 134-141, (1991).
5. Iswar Das, A. Shoeb, Ansari, Nanomaterials in science and technology, J. Scinti.Indus.Res, 68, 657, (2009).
6. Alagarasi, Introduction to Nanomaterials, Introduction to Nanomaterials, pp.76, (2011).
7. http://www.news-medical.net.
8. https://www.conted.ox.ac.uk.
9. www.epa.gov.
10. N. Taniguchi, On the Basic Concept of Nano Technology, Proc. Intl. Conf. Prod. Eng. Tokyo, Part II, Japan Society of Precision Engineering, (1974).
11. Z David, H. Guston, Encyclopedia of nanoscience and society, 1st ed, SAGE publications, 1-1024, (2010).
12. P. Xu, Z.Q.P. Lu, A. Yu, Inorganic nanoparticles as carrriers for efficient cellular delivery, Chemical Engineering Science, 61, 1027-1040. (2006).
13. www.nano.gov.in.
14. B. Paulchamy, G. Arthi, B.D. Lignesh, A simple approach to stepwise synthesis of graphene oxide nanomaterials, J. Nanomed Nanotechnol, 6, 1-4, (2015).

15. Ning Cao, Yuan Zhang, Study of reduced graphene oxide preparation by Hummer's method and related characterization, Journal of Nanomaterials, 2015, 168125, 1-5, (2015).

16. Deepak Kumar Gupta, Rajveer Singh Rajaura, Kananbala Sharma, Int. J. Env. Sci. Technol, 11, 16-24, (2015).

17. Foo Wah Low, Chin Wei Lain, Sharifah Bee Abd Hamid, Easy preparation of ultrathin reduced graphene oxide sheets at high stirring speed, Ceramics International, 41, 5798-5806, (2015).

18. Jianguo Song, Xinzhi Wang, Chang-Tang Chang, Preparation and characterization of graphene oxide, Journal of Nanomaterials, 2014, 276143, 1-6, (2014).

19. Dipanwita Majumdar, Majumdar, Sonochemical synthesized beta-cyclodextrin functionalized graphene oxide and is efficient role in adsorption of water soluble brilliant green dye, J. Environ. Anal. Toxicol, 6, 1-7, (2016).

20. Shanshan wang, Yang Li, Xiaobin fan, Fengbao zhang, Guoliang zhang, β-Cyclodextrin functionalized graphene oxide: an efficient and recyclable adsorbent for the removal of dye pollutants, Front. Chem. Sci. Eng. 1-7, (2014).

21. Ming Chen, Yang Meng, Wang Zhang, Jun Zhou, Ju Xie, Guowang Diao., Electrochimica Acta, 108, 1-9, (2013).

22. Yujing Guo, Shaojun Guo, Jiangtao Ren, Yueming Zhai, Shaojun Dong, Erkang Wang, Cyclodextrin functionalized graphene nanosheets with high supramolecular recognition capability: synthesis and host-guest inclusion for enhanced electrochemical performance, ACS Nano, 4, 4001-4010, (2010).

23. Abolfazl Heydari, Hassan Sheibanic, Facile polymerization of β-cyclodextrin functionalized graphene or graphene oxide nanosheets using citric acid crosslinker by in-situ melt polycondensation for enhanced electrochemical performance, RSC. Adv, 6, 96121-96137, (2016).

24. H. Huawen, H. John Xin, H. Hong, Xiaowen Wang, Xinkun Lu, Organic liquids-responsive β-cyclodextrin-functionalized graphene-based fluorescence

probe: label-free selective detection of tetrahydrofuran, Molecules, 19, 7459-7479, (2014).

25. Yaping Ding, Zhen Zhang, Suqing Gu, Mild and novel electrochemical preparation of β-cyclodextrin/graphene nanocomposite film for super sensitive sensing of quercetin, Biosensors & Bioelectronics, 57, 239-244, (2014).

26. Song Jie Qiao, Xiang Nan Xu, Yang Qiu, Simultaneous reduction and functionalization of graphene oxide by 4-Hydrazinobenzenesulfonic acid for polymer nanocompositesm, Nanomaterials, 6, 1-29, (2016).

27. R. Manash Das, K. Rupak Sarma, Ratul Saiki, S. Vinayak Kale, V. Manjush Shelke, Pinaki Sengupt, Synthesis of silver nanoparticles in an aqueous suspension of graphene oxide sheets and its antimicrobial activity, Colloids and Surfaces B: Biointerfaces, 83, 16-22, (2011).

28. Soumen Dutta, Chaiti Ray, Sougata Sarkar, Mukul Pradhan, Yuichi Negishi, Tarasankar Pal, Silver nanoparticle decorated reduced graphene oxide (rGO) nanosheet: a platform for SERS based low-level detection of uranyl ion, ACS. Appl. Mater. Interfaces, 5, 8724-8732, (2013).

29. Xiu Zhi Tang, Xiaofeng Li, Zongwei Cao, Jinglei Yang, Huan Wang, Xue Pu, Zhong-Zhen Yu, Synthesis of graphene decorated with silver nanoparticles sby simultaneous reduction of grpahene oxide and silver ions with glucose, Carbon, (2013).

30. Khaled Habib, P. Dina, P. Bracho-Rincon, A. Jose Gonzalez Feliciano, C. Juan Villalobos Santos, I. Vladimir Makarov, Darinel Ortizd, A. Javier Avalos, I. Carlos Gonzalez, R. Brad Weiner, Gerardo Morell, Synergistic antibacterial activity of PEGlayted silver-graphene quantum dots nanocomposites, Applied Materials Today, 1, 80–87, (2015).

31. Ana Carolina Mazarin de Moraes, Bruna Araujo Lima, Andreia Fonseca de Faria, Marcelo Brocchi, Oswaldo Luiz Alves, Graphene silver nanocomposite as a promising biocidal agent against methicilin resistant staphylococcus aureus International Journal of Nanomedicine, 10, (2015).

32. Guoqi Feng, Qiang Gan, Hairu Shang, Changgen Feng, 4th International Conference on Mechatronics, Materials, Chemistry and Computer Engineering, (2015).

33. Selvakumar Palnisamy, Balamurugan Tirumalaraj, Sayee Kannan Ramaraj, A Facile electrochemical preparation of reduced graphene oxide@polydopamine composite: A novel electrochemical sensing platform for amperometric detection of chloropromazine, Scientific Reports, 6, (2016).

34. Wenjing Hong, Hua Bai, Yuxi Xu, Zhiyi Yao, Zhongze Gu, Gaoquan Shi, J. Phys. Chem. C, 114, 1822-1826, (2010).

35. Wenbei Zhang, Jiuli Chang, Jianhua Chen, Fang Xu, Feng Wang, Kai Jiang, Zhiyong Gao, Gaphene-Au composite sensor for electrochemical detection of para-nitrophenol, Res Chem Intermed, 38, 2443–2455, (2012).

36. Ping Li, Xudong Chen, Jian-Bing Zeng, Lin Gan, Ming Wang. RSC Adv, 6, 5784-5791, (2016).

37. Kuo yuan Hwa, B. Subramani, Biosens. Bioelectron, 15, 127-133, (2014).

38. Murugan Saranya, Rajendran Ramachandran, Fei Wang, Journal of Science: Advanced Materials and Devices, 1, 454-460, (2016).

39. Xuan Zhang, Yi Chi Zhang, Li Xia Ma, One-pot facile fabrication of graphene-zinc oxide composite and its enhanced sensitivity for simultaneous electrochemical detection of ascorbic acid, dopamine and uric acid, Sensors and Actuators B, 227, 488-496, (2016).

40. Qiwen Chen, Luyan Zhang, Gang Chen, Facile Preparation of Graphene-Copper Nanoparticle Composite by in Situ Chemical Reduction for Electrochemical Sensing of Carbohydrates, Anal. Chem, 84, 171-178, (2012).

41. Wei Wu, Bao Wang, Yu Guo, Synthesis of CuO/graphene nanocomposite as a high-performance anode material for lithium-ion batteries, J. Materials Chemistry, 20, 10661-10664, (2010).

42. Jaewon Hwang, Dong Jin Yoo, Science of Advanced Materials, 7, 329-336, (2015).

43. Ting Hu, Lie Chen, Kai Yuan, Yiwang Chen, Chem. Eur. J, 20, 17178-17184, (2014).

44. Junwei Ding, Shiying Zhu, Tao Zhu, Wei Sun, Qing Li, Gang Wei, Zhiqiang Su, RSC Adv, 5, 22935-22942, (2015).

45. H.O. Pierson, Handbook of carbon, graphite, diamonds and fullerenes: processing, properties and applications: William Andrew, (2012).

46. Z. Ren, Y. Lan, Y. Wang, Aligned carbon nanotubes, Springer-Verlag Berlin Heidelberg, (2013).

47. C.H. Lui, Li Lu, K.F. Mak, W. George Flynn, Ultra flat graphene, Nature, 462, 339-341, (2009).

48. www.aznano.com

49. C. Gomez Navarro, Marko Burghard, Klaus kers, Elastic properties of chemical derived single graphene sheets, Nano Letters, 10, 1144-1148, (2010).

50. D. Pandey, R.Reifenberger, R.Piner, Scanning probe microscopy study of exfoliated oxidized graphene sheets, Surface. Science, 602, 1607-1613, (2008).

51. L. Staudenmaier, Verfahren zur darstellung der graphitsaure, Berichte der deutschen chemischen Gesellschaft, 31, 1481-1487, (1898).

52. D.R. Dreyer, S. Park, C.W. Bielawski, R.S. Ruoff, The chemistry of graphene oxide, Chemical Society Reviews, 39, 228-240, (2010).

53. J.R. Hummers, W.S Offeman, Preparation of graphitic oxide, American Chemical Society, 80, 1339-1339, (1958).

54. S. Basu, P. Bhattacharyya, Recent developments on graphene and graphene oxide based solid state gas sensors, Sens. Actuators, B, 173, 1-21, (2012).

55. S. Park, K.S. Lee, G. Bozoklu, W. Cai, S.T. Nguyen, R.S. Ruoff, ACS Nano, 2, 572-578, (2008).

56. S. Stankovich, R.D. Piner, S.T. guyen, R.S. Ruoff, Graphene oxide papers modified by divalent ions-enhancing mechanical properties via chemical cross-linking, Carbon, 44, 3342-3347, (2006).

57. J. Parades, S. Villar Rodil, A. Martinez Alonso, J.M.D. Tascon, Graphene Oxide Dispersions in Organic Solvents, Langmuir, 24, 10560- 10564, (2008).

58. S. Park, R.S. Ruoff, Chemical methods for the production of graphenes, Nat. Nanotechnol, 4, 217-224, (2009).

59. K.S. Novoselov, A.K, Geim, S.V. Morozov, D. Jiang, Electric Field Effect in Atomically Thin Carbon Films, Science, 306, 666-669, (2004).

60. C.H. Lui, Li Lu, Kin Fai Mak, W. George, Ultraflat graphene, Nature, 462, 339-341, (2009).

61. H.C. Schniepp, Je Luen Li, J. Michael Mc Allister, Hiroaki Sai, Margarita Herrera Alonso, Functionalized Single Graphene Sheets Derived from Splitting graphite Oxide, J. Phys. Chem. B, 110, 8535-8539, (2006).

62. J.I. Paredes, S. Villar Rodil, P. Solis Fernadez, A. Martinez Alonso, Atomic force and scanning tunneling microscopy imaging of graphene nanosheets derived from graphite oxide, Langmuir, 25, 5957-5968, (2009).

63. K.A. Mkhoyan, W. Alexander Contryman, John Silx, A. Derek Stewarts, Nano Lett, Atomic and electronic structure of graphene-oxide, 9, 1058-1063, (2009).

64. K.N. Kudin, Bulent Ozbas, C. Hannes Schniepp, K. Rober Prudhomme, Nano Lett, Raman spectra of graphite oxide and functionalized graphene sheets, 8, 36-41, (2007).

65. C. Gomez Navarro, R. Thomas Weitz, M. Alexander Bitter, Matteo Scolari, Electronic transport properties of individual chemically reduced graphene Oxide sheets, Nano Lett, 7, 3499-3503, (2007).

66. Q. Zheng, Z. Li, J. Yang, J.K. Kim, Graphene oxide-based transparent conductive films, Progress in Materials Science, 64, 200-247, (2014).

67. I. Jung, D.A. Dikin, R.D. Piner, R.S. Ruoff, Tunable electrical conductivity of individual graphene oxide sheets reduced at low temperatures, Nano Lett, 8, 4283-4287, (2008).

68. S.J. Wang, Y. Geng, Q. Zheng, J.K. Kim, Fabrication of highly conducting and transparent graphene film, Carbon, 48, 1815-1823, (2010).

69. J.W. Suk, R.D. Piner, J. An, R.S. Ruoff, Mechanical properties of monolayer graphene oxide, ACS Nano, 4, 6557-6564, (2010).

70. Q. Zheng, Y. Geng, S. Wang, Z. Li, J.K Kim, Effects of functional groups on the mechanical and wrinkling properties of graphene sheets, Carbon, 48, 4315-4322, (2010).

71. G. Eda, Yun Yue Lin, Cecilia Mattevi, Hisato, Yamaguchi, Hsin An Chen, Chemically derived graphene oxide: towards large-area thin- film electronics and optoelectronics, Adv. Mater, 22, 2392-2415, (2010).

72. C.H. Li Lu, Kin Fai Mak, W. George, Ultraflat graphene, Nature, 462, 339-341, (2009).

73. C.H. Huang, Ho Ki, J.H. Liao, W. Zhang, J. Li, Sci. Rep, 4, 1-7, (2014).

74. H. Bai, C. Li, G. Shi, Functional composite materials based on chemically converted graphene, Adv. Mater, 23, 1089, (2011).

75. Y. Shao, J. Wang, H. Wu, J. Liu, I.A. Aksay, Y. Lin Y, Graphene based electrochemical sensors and biosensors: A Review, Electroanalysis, 22, 1027-1036, (2010).

76. Q. He, S. Wu, Z. Yin, H. Zhang, Graphene-based electronic sensors, Science, 3, 1764-1772, (2012).

77. V. Georgakilas, M. Otyepka, A.B. Bourlinos, V. Chandra, N. Kim, K.C. Kemp, P. Hobza, R. Zboril, K.S. Kim, Functionalization of graphene: covalent and non-covalent approaches, derivatives and applications, Chem. Rev, 112, 6156-6214, (2012).

78. X. Wang, S. Gaoquan, Flexible graphene devices related to energy conversion and storage, Energy Environ. Sci, 8, 790-823, (2015).

79. H. Ping, M. Zhang, M, Li H, Li S, Chen Q, Sun C, Zhang T. Visual detection of melamine in raw milk by label-free silver nanoparticles, Food Control, 23, 191-197, (2012).

80. M. Zhang, X. Cao, H. Li, F. Guan, J. Guo, F. Shen, Y. Luo, C. Sun, L. Zhang, Sensitive fluorescent detection of melamine in raw milk based on the inner filter effect of Au nanoparticles on the fluorescence of CdTe quantum dots, Food Chemistry, 135, 1894-1900, (2012).

81. M. Yun, J.E. Choe, J.M. You, M.S. Ahmed, J. Lee, High catalytic activity of electrochemically reduced graphene compositetoward electrochemical sensing of Orange II, Food Chemistry, 169, 114-119, (2015).

82. Q. Xi, X. Chen, D.G. vans, W. Yang, Gold nanoparticle-embedded porous graphene thin films fabricated via layer-by-layer self-assembly and subsequent thermal annealing for electrochemical sensing, Langmuir, 28, 9885-9892, (2012).

83. L. Zhong, S. Gan, X. Fu, F. Li, D. Han, Cost-effective three-dimensional graphene/Ag aerogel composite for high-performance sensing, Electrochimica Acta, 89, 222-228, (2013).

84. Y. Liu, Q. Chang, L. Huang, Journal of Material Chemistry C, 1, (2013).

85. T.D. Dao, J.E. Hong, K.S. Ryu, H.M. Jeong, Super-tough functionalized graphene paper as a high capacity anode for lithium ion batteries, Chemical Engineering Journal, 250, 257-266, (2014).

86. R. Stephan belding, W. Fallyn campbell, J.F. Edmund dickinson, G. Richard compton, Nanoparticle-modified electrodes, Physical chemistry chemical physics, 12, 11208-11221, (2010).

87. W.M. Compton, Y.F. Thomas, F.S. Stinson, B.F. Grant, Arch. Gen. Psychiatry, 64, 566-576, (2007).

88. D. Belanger, Pinson, Electrografting: a powerful method for surface modification, Chem. Sov. Rev, 40, 3995-4048, (2011).

89. www.cd-bioparticles.com

90. Jiang, Zhong jie, Liu, Chun yan, Sun, Lu wei, Catalytic properties of silver nanoparticles supported on silica spheres, The journal of physical chemistry B, 109, 1730-1735.

91. J.C. Pickup, Z.L. Zhi, F. Khan, T. Saxi, D.J. Birch, Diabetes metab res.rev, 24, 604-610, (2008).

92. www.wikipedia.com

93. M. Zhng, C. Hou, A. Halder, Q. Chi, Nanomedicine and its potential in diabetes research and practice, ACS Applied Materials Interfaces. 9, 3922-3930, (2017).

94. X.C. Dong, H. Xu, X.W. Wang, Y.X. Huang, M.B. Chan Park, H. Zhang, L.H. Wang, W. Huang, 3D Graphene-cobalt oxide electrode for high-performance supercapacitor and enzymeless glucose detection, ACS Nano, 6, 3206-3213, (2012).

95. Jayanta Kumar Behera, M.Tech Thesis, NIT Rourkela.

96. http://www.znoxide.org/properties.html

97. www.chemibook .com

98. Zhong Lin Wang, Nanostructures of zinc oxide, Materials Today, 7, 26-33, (2004).

99. H. Wayne Richardson, Copper compounds, Wiley-VCH, Weinheim, (2002).

100. www.nanoparticles-microsphere.com.

101. J.B. Forsyth, S. Hull, The effect of hydrostatic pressure on the ambient temperature structure of CuO, J. Phys. Condens. Matter 3, 5257-5261, (1991).

102. R. Agarwal, V. Gupta, Cyclodextrins-A review on pharmaceutical application for drug delivery, IJPR, 2, 95-112, (2012).

103. M.E. Davis, M.E. Brewster, Cyclodextrin-based pharmaceutics: past, present and future, Nature reviews, 3, 1023-35, (2004).

104. A. Kumar, R. Verma, S. Purohit, A. Bhandhari, J Natura Conscientia, 2, 293-305, (2011).

105. T. Loftsson, D. Duchene, Cyclodextrins and their pharmaceutical applications, Int J Pharm, 329, 1-11, (2007).

106. A. Villiers, Compt. Rend. Acad. Sci, 112, 536-538, (1891).

107. S.D. Eastburn, B.Y. Tao, Applications of modified cyclodextrins, Biotechnol Adv, 12, 325–339, (1994).

108. R. Challa, A. Ahuja, J. Ali, Cyclodextrins in drug delivery: An updated review, AAPS Pharm. Sci. Tech, 6, 329-357, (2005).

109. T. Loftsson, M.E. Brewster, Pharmaceutical applications of cyclodextrins. Drug solubilization and stabilization, J Pharm Sci. 85, 1017-1025, (1996).

110. Leuner C, Dressman, Improving drug solubility for oral delivery using solid dispersions, Eur. J. Pharm. Bio, 50, 47-60, (2000).

111. M.E. Brewster, Cyclodextrins as pharmaceutical solubilizers. advanced drug delivery reviews, Adv Drug Del Reviews, 59, 645-666, (2007).

112. Mamoru Kmaiya, Setsuko Mitsuhashi, Masakazu Makino, Catalytic properties of cyclodextrins on the hydrolysis of parathion and paraoxon in aquatic medium containing humic acids, Chemosphere, 25, 1783-1796, (1992).

113. Masateru Taniguchi, Tomoji Kawai, Effect of α-cyclodextrin coating on electronic properties of molecular wires, Chemical Physics Letters, 431, 127-131, (2006).

114. Mouna Bouzitoun, Cherif Dridi, Hafedh Ben Quada, Science and Technology of Advanced Materials, 7, 772-779, (2006).

115. Nan Zhou, Xia Shi zhu, Ionic liquids functionalized β-cyclodextrin polymer for separation/analysis of magnolol, J. Pharmaceutical Analysis, 4, 242-249, (2014).

116. M. Diego, Alzate Sanchez, Brian Smith, P. Juan, 28, 8340-8346, (2016).

117. Christian Folch, M. Yazdani Perdram, Claudio Olea Azar, Inclusion and functionalization of polymers with cyclodextrins: current applications and future prospects, Molecules, 19, 14066-14079, (2014).

118. G. Liu, W. Jin, N. Xu, Graphene based memberanes, Chemical Society Review, 44, 5016-5030, (2015).

119. Y. Shao, M.F. El Kady, L.J. Wang, Q. Zhang, Y. Li, H. Wang, Graphene-based materials for flexible supercapacitors, Chemical Society Review, 44, 3639-3665, (2015).

120. M.S.P. Sha, A.R. Boccaccini, Applications of graphene electrophoretic deposition. A review, Physical Chemistry B, 117, 1502-1515, (2012).

121. M. Zhang, C. Hou, A. Halder, Graphene papers: smart architecture and specific functionalization for biomimetics, electrocatalytic sensing and energy storage, Materials Chemistry Frontiers, 1, 37-60, (2017).

122. Y. Zhang, J. Shen, H. Li, The Chemical Record, 16, 273-294, (2016).

123. A. Halder, M. Zhang, Q. Chi, Electroactive and biocompatible functionalization of graphene for the development of biosensing platforms, Biosensors and Bioelectronics, 87, 764-771, (2017).

124. L. Luo, L. Zhu, Z. Wang, Bioelectrochemistry, 88, 156-163, (2012).

125. W. Gao, Y. Chen, J. Xi, S. Lin, Y. Chen, Y. Lin, A novel electrochemiluminescence ethanol biosensor based on tris(2,2′-bipyridine) ruthenium (II) and alcohol dehydrogenase immobilized in graphene/bovine serum albumin composite film, Biosensors and Bioelectronics, 41, 776-782, (2013).

126. L.E. Delle, C. Huck, M. Backer, Applied Materials Science, 212, 1327-1334, (2015).

127. B.C. Smith, Fundamentals of Fourier transform infrared spectroscopy. 2nd ed. Boca Raton, FL: CRC Press, (2011).

128. A.R. Hind, S.K. Bhargav, A. Mc Kinnon, At the solid liquid interface: FT-IR/ATR the tool of choice, Advances in Colloid and Interface Science, 93, 91-114, (2001).

129. www. Britannica.com.

130. W. Bragg, The Diffraction of Short Electromagnetic Waves by Crystals, proceedings of the Cambridge Philosophical Society, 1-4, (1913).

131. M. J. Wilson, X-ray powder diffraction methods." A handbook of determinative methods in clay mineralogy, 26-98, (1987).

132. L. Ooi, Principles of X-ray Crystallography. Oxford University Press, (2010).

133. J.J. Bozzola, Jones, Bartlett, Electron Microscopy: Principles and Techniques for Biologists, Published by The Jones and Bartlett Series in Biology, (1992).

134. W.F. Smith, W.F. and J. Hashemi, 5th ed. 2010, Boston, Mass.: McGraw-Hill. xviii, 1068 p.

135. M.A. Joshi, Bhattacharyya, S.W. Ali, Characterization techniques for nanotechnology applications in textiles, Indian Journal of Fiber and Textile Research, 33, 304-317, (2008).

136. M.I. Szynkowska, 3rd edition, In Encyclopedia of Analytical Science, (2005).

137. J. Goldstein, D.E. Newbury, D.C. Joy, C.E. Lyman, P. Echlin, E. Lifshin, Scanning Electron Microscopy and X-ray Microanalysis, 3rd ed, Springer, (2003).

138. N. Kanani, Electroplating, 1st edition, Elsevier Science, (2005).

139. http://www.dstuns.iitm.ac.in/microscopy-instruments.php.

140. www.toppr.com.

141. https://ecs.confex.com.

142. https://chem.libretexts.org.